Molecular Interactions of Nonpeptide Agonists and Antagonists with the Melanocortin-4 Receptor

Beth A. Fleck,[‡] Chen Chen,[§] Weidong Yang,[||] Rajesh Huntley,[‡] Stacy Markison,[⊥] Sarah A. Nickolls,[||] Alan C. Foster,[⊥] and Sam R. J. Hoare*[,‡]

Departments of Pharmacology, Medicinal Chemistry, Molecular Biology, and Neuroscience, Neurocrine Biosciences Inc., 12790 El Camino Real, San Diego, California 92130

Received July 8, 2005; Revised Manuscript Received August 10, 2005

ABSTRACT: The melanocortin-4 (MC4) receptor is a potential therapeutic target for obesity and cachexia, for which nonpeptide agonists and antagonists are being developed, respectively. The aim of this study was to identify molecular interactions between the MC4 receptor and nonpeptide ligands, and to compare the mechanism of binding between agonist and antagonist ligands. Nonpeptide ligand interaction was affected by mutations that reduce peptide ligand binding (D122A, D126A, S190A, M200A, F261A, and F284A), confirming overlapping binding determinants for peptide and nonpeptide ligands. The common halogenated phenyl group of nonpeptide ligands was a determinant of F261A and F284A mutations' affinity-reducing effect, implying this group interacts with the aromatic side chains of these residues. All affected compounds contain this group, the mutations reduced binding of 2,4-dichloro-substituted compounds more than 4-chloro-substituted-compounds, and F284A mutation eliminated the affinity-enhancing effect of 2-chloro-substitution. F261A and F284A mutations reduced the affinity of antagonists more than agonists, suggesting that the stronger ligand interaction with these residues, the lower the ligand efficacy. Supporting this hypothesis, F261A mutation increased the efficacy of nonpeptide antagonist and partial agonist ligands. D122A and D126A mutations reduced nonpeptide ligand interaction. Removing the ligands' derivatized amide group eliminated the effect of the mutations. Interaction of agonists, which bear a common amine within this group, was strongly reduced by D126A mutation (550−3300-fold), suggesting an electrostatic interaction between the amine and the acidic group of D126. These postulated interactions with aromatic and acidic regions of the MC4 receptor are consistent with a molecular model of the receptor. Furthermore, the strength of interaction with the aromatic pocket, and potentially the acidic pocket, controls the signaling efficacy of the ligand.

The melanocortin (MC)[1] system comprises a family of five G-protein coupled receptors (GPCRs) [MC1−MC5 receptors (*1*−*3*)] that are regulated by endogenous peptide agonists and antagonists. The three agonists, α-melanocyte-stimulating hormone (α-MSH), γ-MSH, and adrenocorticotropin hormone, are derived from the precursor peptide pro-opiomelanocortin (*4*−*6*). The two endogenous antagonists are agouti (*7*) and agouti-related protein (AgRP) (*8*, *9*). The MC4 receptor has been implicated in the regulation of feeding and metabolism as well as erectile function (*6*, *10*, *11*). MC4 receptor agonists can suppress food intake and body weight in rodents (*12*−*16*), promote penile erection in rodents (*16*, *17*) and man (*18*), and facilitate sexual solicitation in female rats (*19*). MC4 receptor antagonists can increase feeding and induce body weight gain in rodents (*20*−*22*). On the basis of these findings, MC4 receptor agonists are being developed as potential treatments for obesity or erectile dysfunction. The former disease indication is strongly supported by mouse and human genetic studies (*23*, *24*). MC4 antagonism has been proposed for treatment of cachexia, a wasting disorder associated with chronic disease states such as cancer and renal failure (*25*, *26*).

The mechanisms of peptide ligand binding to the MC4 receptor have been studied in detail using structure−activity relationships (SAR) of the peptide ligands (*27*) and mutagenesis of the receptor (*28*−*32*). The endogenous peptide agonists α-MSH, γ-MSH, and adreocorticotropin hormone share a His-Phe-Arg-Trp sequence (*27*). The His-Phe-Arg-Trp fragment potently activates the MC4 receptor (*33*). Substitution of L-Phe[7] of α-MSH with D-Phe increases binding affinity for the melanocortin receptors (*33*, *34*), yielding the nonselective high-affinity agonist NDP-MSH ([Nle[8], D-Phe[7]]α-MSH (*34*)). Moderately MC4 selective agonists have been developed by cyclization around His-Phe-Arg-Trp or Phe-Arg-Trp motifs (*27*), together with further SAR optimization [e.g., MTII (Ac-Nle-c[Asp-His-D-Phe-Arg-Trp-Lys]-NH_2 (*35*, *36*)]. Antagonists have been

* To whom correspondence should be addressed. Department of Pharmacology, Neurocrine Biosciences Inc., San Diego CA 92130. Tel.: 858-617-7678; Fax: 858-617-7830. E-mail: shoare@neurocrine.com.

[‡] Department of Pharmacology.

[§] Department of Medicinal Chemistry.

[||] Department of Molecular Biology.

[⊥] Department of Neuroscience.

[1] Abbreviations: AgRP, agouti-related protein; DPBS, Dulbecco's phosphate-buffered saline; GPCR, G-protein-coupled receptor; MC, melanocortin; MSH, melanocyte-stimulating hormone; SAR, structure−activity relationship; Tic, *R*-1,2,3,4-tetrahydoisoquinolin-3-ylcarbonyl; TM, transmembrane domain; WT, wild-type.

10.1021/bi051316s CCC: $30.25
Published on Web 10/14/2005

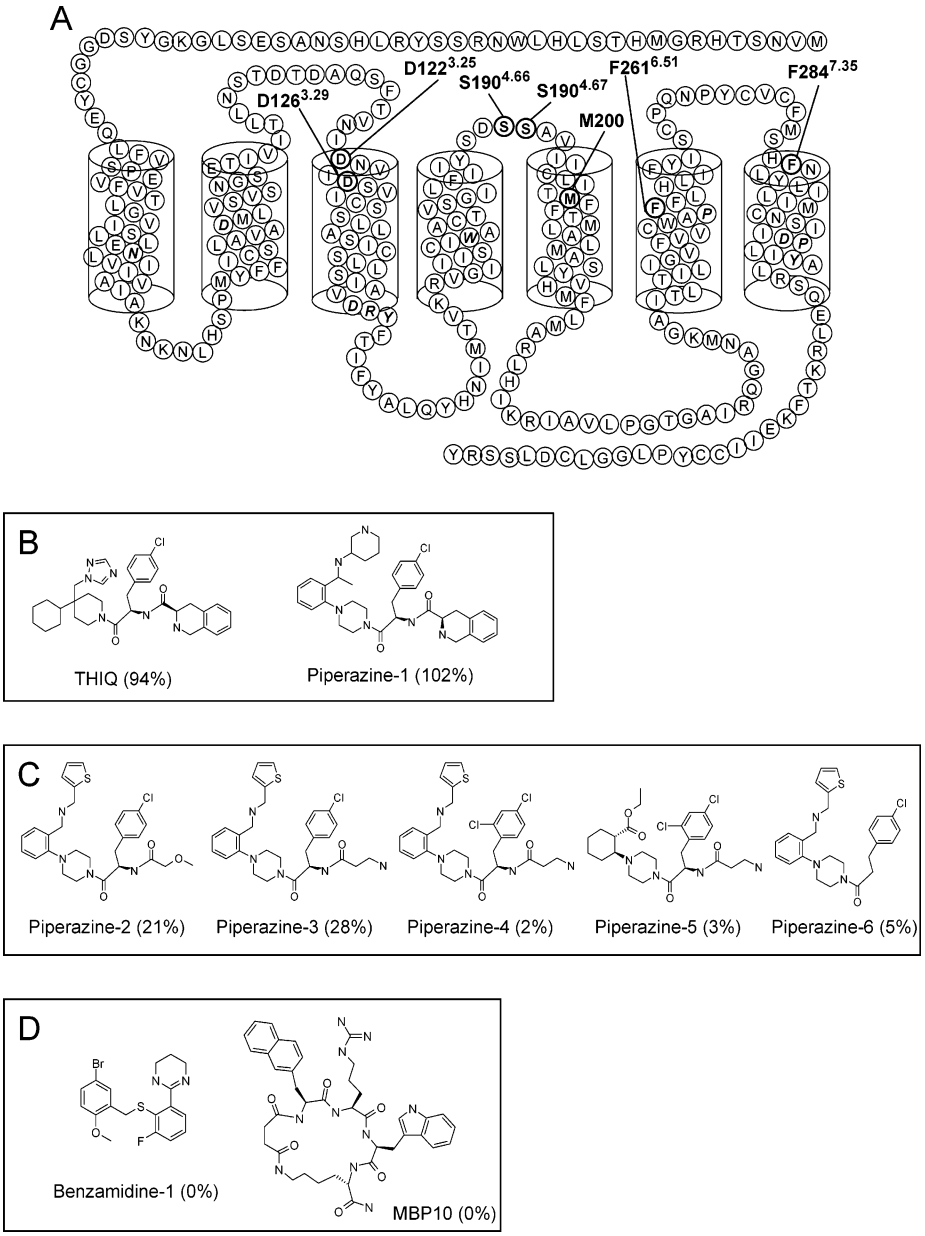

FIGURE 1: Molecular properties of the MC4 receptor and nonpeptide ligands. (A) Topographical representation of the human MC4 receptor amino acid sequence, indicating position of mutated residues. Residues mutated in this study are indicated by bold font in bold circles. Residues indicated in bold italic type represent residues conserved within rhodopsin-like GPCRs. Note that the MC4 receptor lacks a highly conserved cysteine in extracellular loop 2, a residue in rhodopsin and potentially most rhodopsin-like receptors that forms a disulfide bond with a cysteine in TM3 (*57*−*59*). Also note that the conserved **N**PXXY motif in TM7 of Class A GPCRs (*59*) is replaced with the **D**PLIY motif in the MC4 receptor. The MC4 receptor also lacks the conserved proline in TM5 (*59*). Residues are numbered by their position in the sequence of the human MC4 receptor and, in superscript, according to the indexing method of Ballesteros and Weinstein (*61*). (B) Chemical structure of nonpeptide agonist ligands. [See ref *16* for THIQ and ref *43* for piperazine-1.] (C) Chemical structure of piperazine partial agonist/antagonist ligands. (See ref *42* for piperazine-2 and piperazine-3, ref *39* for piperazine-4, ref *52* for piperazine-5, and ref *42* for piperazine-6.) (D) Chemical structure of the nonpeptide antagonist benzamidine-1 (*20*) and the small peptide antagonist MBP10 (*38*). The numbers in parentheses are the E_{max} values for stimulation of cAMP accumulation in HEK cells expressing the human MC4 receptor, expressed as a percentage of the NDP-MSH E_{max}. Values for THIQ and piperazines 1−4 are from Table 4, the value for piperazine-5 is the effect for a 10 μM concentration from ref *52*, and the values for piperazine-6, benzamidine-1, and MBP10 are for 10, 10, and 100 μM concentrations, respectively (data not shown).

developed by substitution of the Phe[7] phenyl side chain with larger aromatic groups, e.g., SHU9119 [in which D-Phe of MTII is replaced with D-Nal(2′) (*37*) and MBP10 Ac-c[Suc-D-Nal(2′)-Trp-Lys]-NH_2 (*38*), Figure 1D]. Two regions of the receptor have been identified as critically involved in peptide binding (*28*−*32*): (i) an acidic pocket of negatively charged residues in transmembrane domains (TMs) 2 and 3 (E100, D122A, and D126A, Figure 1A); (ii) a putative hydrophobic pocket formed from aromatic or bulky residues in TM4 (F184 and Y187), TM6 (F261, F262, H264, and F267), and TM7 (F284) (Figure 1A). Arg[8] of NDP-MSH has been proposed to interact with D122 and D126 (*28*, *29*), and Phe[7] likely interacts with the putative hydrophobic cage (*28*).

Numerous nonpeptide agonists and antagonists have been developed for the MC4 receptor (*12*, *16*, *20*, *27*, *39*−*46*). Potent MC4-selective agonists generally possess a substituted benzene ring (such as the 4-chlorophenyl group of THIQ, Figure 1B), adjacent to an amine-containing group on the

"right-hand side" as drawn in Figure 1 [such as the *R*-1,2,3,4-tetrahydoisoquinolin-3-ylcarbonyl (Tic) group of THIQ and piperazine-1, Figure 1B]. The left-hand side is generally comprised of bulky cyclic groups, with 2-position side chains that frequently confer higher affinity for the MC4 receptor compared with other melanocortin receptors. Two classes of potent MC4 selective antagonists have been reported. The first class is similar in general structure to the agonist compounds (e.g., piperazines-4 and -5, Figure 1B), and the second class comprises a series of benzamidines (e.g., benzamidine-1, Figure 1C) and closely related benzamidazoles (*20*, *47*). Regions and residues of the MC4 receptor that act as determinants of nonpeptide ligand binding have been identified. Proteochemical mapping of nonpeptide ligand binding to wild-type and chimeric melanocortin receptors indicated the importance of broadly defined regions of the MC4 receptor in nonpeptide ligand binding (*48*, *49*). At a higher resolution, three MC4 receptor mutations that affect binding of α-MSH (D122A, F261A, and F284A) also reduce affinity of THIQ, implying overlapping binding sites for peptide and nonpeptide agonists (*30*). Specific molecular interactions between binding determinants of nonpeptide ligand and amino acid side chains of the receptor have only been explored indirectly, and the findings are currently inconsistent. Superposition of the nonpeptide agonist THIQ (*16*) on peptide ligand is consistent with the substituted aromatic group of the former mimicking Phe^7 of the latter (the residue that binds within the hydrophobic cage). The Tic group of THIQ is oriented close to His^6 in one superposition (*16*), whereas in a second the Tic amine lies close to Arg^8 (*40*) (the residue that binds within the acidic pocket). Molecular modeling of the MC4 receptor interaction with THIQ or a close analogue suggests that the amine functionality of the Tic group interacts with the acidic pocket (*50*, *51*). In one model, the left-hand side of the molecule is oriented within the hydrophobic cage (*51*), whereas in a second model the 4-chlorophenyl group lies in this position (*50*).

None of the putative interactions between nonpeptide ligands and the MC4 receptor have been tested directly, and little is known of the mechanistic differences between nonpeptide agonist and antagonist binding. In this study, we used site-directed mutagenesis combined with ligand SAR with the aim of identifying molecular interactions between specific groups of nonpeptide ligand and amino acid side chains of the MC4 receptor. This evaluation included the use of multiple piperazine ligands with discrete structural differences (Figure 1B,C) to allow us to identify the structural determinants of the ligand underlying the mutations' effects. We also tested the smaller, structurally distinct antagonist benzamidine-1 (Figure 1D). This test set of ligands also possessed varying efficacy for activation of the MC4 receptor (Figure 1B−D), allowing us to identify the relative role of receptor and ligand determinants in MC4 receptor activation.

EXPERIMENTAL PROCEDURES

Materials. Human α-MSH and NDP-MSH were purchased from Bachem (Torrance, CA). Human AgRP(83−132), the bioactive fragment of AgRP (*8*), was purchased from Phoenix Pharmaceuticals (Belmont, CA). MBP10 (Ac-c[Suc-D-Nal-(2′)-Trp-Lys]-NH_2) (*38*) was synthesized by solid-phase methodology on a Beckman Coulter 990 peptide synthesizer (Fullerton, CA) using t-Boc-protected amino acids. The assembled peptide was deprotected with hydrogen fluoride and purified by preparative HPLC. The purity of the final product was assessed by analytical HPLC and mass spectrometric analysis using an ion-spray source. Peptides were dissolved in deionized water at a concentration of 1 mM (except AgRP(83−132), 100 μM) and stored in aliquots at −80 °C. Aliquots were used once, and any remaining solution was discarded. Synthesis of nonpeptide ligands (see Figure 1 for chemical structures) was performed as described: ref *16* for THIQ (compound **1** of this reference; *N*-[(3*R*)-1,2,3,4-etrahydroisoquinolinium-3-ylcarbonyl]-(1*R*)-(4-chlorobenzyl)-2-[4-cyclohexyl-4-(1*H*-1,2,4-triazol-1-yl-methyl)piperidin-1-yl]-2-oxoethylamine); ref *43* for piperazine-1 (compound **13g**; 4-{(*2R*)-[1,2,3,4-tetrahydro-(3*R*)-isoquinolinecarboxamido]-3-(4-chlorophenyl)propionyl}-1-{2-[1-(piperidin-3-ylamino)ethyl]phenyl}piperazine); ref *42* for piperazine-2 (compound **11n**; 4-[(*2R*)-(2-methoxyacetamido)-3-(4-chlorophenyl)propionyl]-1-{2-[(2-thienyl) ethylaminomethyl]phenyl}piperazine); ref *42* for piperazine-3 (compound **11c**; 4-[(*2R*)-(3-aminopropionaylmido)-3-(4-chlorophenyl)propionyl]-1-{2-[(2-thienyl)ethylaminomethyl]-phenyl}piperazine); ref *39* for piperazine-4 (compound **10**; 4-[(*2R*)-(3-aminopropionaylmido)-3-(2,4-dichlorophenyl)propionyl]-1-{2-[(2-thienyl)ethylaminomethyl]phenyl}-piperazine); ref *52* for piperazine-5 (compound **12i**; *trans*-2-{4-[(*2R*)-(3-amino-propionylamino)-(3)-(2,4-dichlorophenyl)propionyl]-piperazin-1-yl}cyclohexanecarboxylic acid ethyl ester); ref *42* for piperazine-6 (compound **10f**; 3-(4-chlorophenyl)propionyl]-1-{2-[(2-thienyl)ethylaminomethyl]-phenyl}piperazine); and ref *20* for benzamidine-1 (thiomethyl ether analogue of compound **7**; 2-[2-(5-bromo-2-methoxybenzylsulfanyl)-3-fluorophenyl]-1,4,5,6-tetrahydropyrimidine). Nonpeptide ligands were dissolved in DMSO at a concentration of 6 mM.

[^{125}I]NDP-MSH was from PerkinElmer Life Sciences (Boston, MA) (specific activity of 2200 Ci/mmol). G418 (Geneticin), Dulbecco's phosphate-buffered saline (DPBS) and cell culture supplies were from Invitrogen (Carlsbad, CA). Fetal bovine serum was from HyClone (Logan, UT).

Construction of Mutant Receptors and Expression in HEK293 Cells. The human MC4 receptor cDNA in pcDNA3.1 was used as the template for site-directed mutagenesis, using the QuikChange kit (Stratagene, La Jolla, CA). PCR reactions (95 °C, 1 min; 52 °C, 1 min; and 72 °C, 16 min) were performed using *Pfu* polymerase and a complementary set of primers encoding the nucleotide mutation, resulting in the desired amino acid residue change. Template DNA was nicked with *Dpn*I, and mutant DNA was subcloned into competent TOP10 cells. Clones were sequenced using an ABI Prism 377 DNA sequencer (Applied Biosystems, Foster City, CA), and clones containing the desired mutation were subcloned into the *Eco*RI/*Xho*I site of a fresh pcDNA3.1 vector. Complete receptor sequences were confirmed by DNA sequencing. Wild-type (WT) or mutant MC4 receptor plasmid cDNA was transfected into HEK293 cells using LipofectAMINE (Invitrogen) according to the manufacturer's protocol. Stable single cell clones were isolated after selection using 1 mg/mL G418 in complete medium (Dulbecco's modified Eagle's medium, supplemented with 10% heat-inactivated fetal bovine serum, 2 mM glutamine, 1 mM sodium pyruvate, 10 mM HEPES, 50 IU/mL penicillin, and 50 μg/mL streptomycin). Stable cell lines were maintained

in 250 μg/mL G418 in complete medium. D122A and M200A mutant MC4 receptors were expressed transiently in HEK293 cells using Polyfect transfection reagent (Qiagen, Valencia, CA) according to the manufacturer's protocol. Cells were collected 2 days after transient transfection for cell membrane preparation.

Preparation of Cell Membranes. Cell membranes were prepared using a high-pressure nitrogen cell and differential centrifugation as previously described (*53*). The lysis buffer was DPBS. The final membrane pellet was resuspended in binding assay buffer (25 mM HEPES, 1.5 mM $CaCl_2$, 1 mM $MgSO_4$, 100 mM NaCl, pH 7.0). The protein concentration in the membrane pellet was determined using the Coomassie method (Pierce, Rockford, IL), using bovine serum albumin as the standard. Membranes were stored at −80 °C before use.

Radioligand Binding Assays. Binding affinity of unlabeled ligands for wild-type and mutant MC4 receptors was measured by displacement of [^{125}I]NDP-MSH binding. The following were added sequentially to low-binding 96-well plates (#3605, Corning, Palo Alto, CA) in binding assay buffer (see *Preparation of Cell Membranes* for recipe): 50 μL of unlabeled ligand, 75 μL of [^{125}I]NDP-MSH, and 75 μL of membrane suspension. The final concentration of [^{125}I]-NDP-MSH was approximately 0.2 nM. The amount of membrane protein added per well was 6 μg for WT, 3 μg for D122A, 8 μg for S190A, 7 μg for S191A, 13 μg for M200A, 9 μg for F261A, and 20 μg for F284A. Total [^{125}I]-NDP-MSH binding (that in the absence of unlabeled ligand) was less than 20% of the total radioligand added. Assay plates were set on a shaker (Titer Plate Shaker, setting 4, Lab-Line Instruments, Melrose Park, IL), and the assay was incubated for 90 min at room temperature. Bound and free radioligand were then separated by rapid filtration, using UniFilter GF/C filters (Packard, Meriden, CT) pretreated with 0.1% polyethylenimine in DPBS, on a UniFilter-96 vacuum manifold (Packard). The filter was then washed three times with 0.2 mL/well 0.01% Triton X-100 in DPBS, and then dried under electric fans for 40 min to 1 h. Following addition of scintillation fluid (50 μL per filter disk, Microscint 20, Packard), scintillation counts were measured in a Packard Topcount NXT. cpm resulting from emission of Auger electrons from ^{125}I were converted to dpm, using the predetermined counting efficiency of 30%. The total amount of radioligand added was measured using a Packard Cobra II gamma counter (78% efficiency). Affinity and binding site capacity of [^{125}I]NDP-MSH was measured in saturation experiments, by incubating varying concentrations of radioligand (30 pM to 3 nM) in duplicate in the absence and in the presence of 10 μM α-MSH, to define total binding and nonspecific binding, respectively, using the binding assay protocol described above.

Measurement of cAMP Accumulation. HEK293 cells were plated 1 day prior to assay on poly-lysine-coated 96-well plates at a density of 5000 cells/well. For assay, the medium was removed, and the cells were washed with 200 μL of DPBS. Following aspiration of DPBS, 75 μL of cAMP assay buffer was added to each well (Dulbecco's modified Eagle's medium without phenol red, supplemented with 2 mM glutamine, 10 mM HEPES, and 1 mM isobutylmethylxanthine). Ligand was then added in a volume of 25 μL of cAMP assay buffer, and the cells were incubated for 30 min at 37 °C in 5% CO_2. In antagonist assays, antagonists were diluted in a solution of the agonist, such that cells were exposed to both ligands simultaneously. Following cell lysis, cAMP was measured by chemiluminescent immunoassay (Tropix cAMP ELISA, Applied Biosystems, Foster City, CA). Cell lysis was achieved by adding 100 μL of the lysis reagent supplied with the immunoassay kit, followed by incubation for 30 min at 37 °C in 5% CO_2.

Data Analysis. Inhibition of [^{125}I]NDP-MSH binding by unlabeled ligands was fitted to a four-parameter logistic equation to determine K_i using XL*fit* (ID Business Solutions Ltd, Emeryville, CA). In this analysis K_i was determined from IC_{50} using the Cheng-Prusoff equation (*54*). The slope factor in the analysis was between 0.8 and 1.2. Radioligand saturation was analyzed using a previously described method (*53*) that takes into account depletion of free radioligand by receptor-specific and nonspecific binding of radioligand, providing an accurate measurement of K_d. This analysis was performed using Prism 3.0 (GraphPad Software, San Diego, CA). Ligand-stimulated or ligand-inhibited cAMP accumulation was analyzed using a four-parameter logistic equation using Prism 3.0 to provide an estimate of EC_{50} or IC_{50}, respectively. Antagonist inhibitory potency (pK_b) in cAMP accumulation assays was determined by measuring the α-MSH dose response for stimulating cAMP accumulation in the absence of antagonist and in the presence of a single concentration of antagonist. pK_b was then calculated using the following equation (*55*):

$$pK_b = \log(EC_{50}'/EC50) - \log[\text{antagonist}]$$

where EC_{50}' is the α-MSH EC_{50} in the presence of antagonist.

Statistical analysis of differences between values was performed by analysis of variance (ANOVA) using Prism 3.0.

RESULTS

Receptor Binding Determinants for Nonpeptide Ligands. The first aim of this study was to identify MC4 receptor determinants of nonpeptide ligand binding using site-directed mutagenesis. Previous studies have suggested that the binding sites for peptide and nonpeptide ligands overlap. In particular, THIQ and α-MSH affinity was reduced by D122A, F261A, and F284A mutations (*30*). This comparison was extended using additional nonpeptide ligands and MC4 receptor mutations. Mutations that have been shown to affect peptide binding were tested for their effect on nonpeptide ligand binding (D122A and D126A in TM3, M200A in TM5, F261A in TM6, and F284A in TM7, Figure 1A). We also tested S190A and S191A mutations in the second extracellular loop (Figure 1A). These two residues were tested since they are potential hydrogen bond donors that could interact with hydrogen bond acceptors of nonpeptide ligands (Figure 1B−D).

We aimed to measure affinity of nonpeptide ligands by displacement of binding of the radiolabeled peptide agonist [^{125}I]NDP-MSH.[2] This radioligand bound wild-type (WT)

[2] Guanine nucleotides did not appreciably affect binding of [^{125}I]-NDP-MSH or of unlabeled agonists or antagonists for the WT receptor in HEK cells,[30] suggesting that G-protein-coupling does not appreciably affect the ligand binding properties of the MC4 receptor in this assay system. For this reason, agonist and antagonist affinity could be reasonably compared using the binding assay.

Table 1: Affinity and Binding Site Capacity of [^{125}I]NDP-MSH for Wild-Type and Mutant MC4 Receptors[a]

receptor	pK_d **K_d, nM**	B_{max}, pmol/mg
wild-type	9.44 ± 0.04 **0.36**	2.0 ± 0.1
D122A	9.63 ± 0.03 **0.24**	0.86 ± 0.13
D126A	no binding	no binding
S190A	9.52 ± 0.04 **0.30**	1.3 ± 0.2
S191A	9.53 ± 0.02 **0.30**	1.9 ± 0.2
M200A	9.55 ± 0.05 **0.28**	0.17 ± 0.01
F261A	9.40 ± 0.04 **0.40**	1.3 ± 0.1
F284A	9.37 ± 0.03 **0.42**	0.72 ± 0.13

[a] [^{125}I]NDP-MSH saturation of wild-type and mutant MC4 receptors in HEK293 membranes was measured as described in Experimental Procedures. The receptors were stably expressed, with the exception of D122A and M200A, which were expressed transiently. The binding site capacity (B_{max}) was quantified as picomoles of receptor per milligram of membrane protein. Data are mean ± range, $n = 2$, where range is the standard deviation divided by the square-root of n.

and mutant receptors (Table 1), with the exception of D126A. (This mutant receptor also did not detectably bind [^{125}I]AgRP and so was assessed using functional assays; see below.) [^{125}I]-NDP-MSH binding was not detected in membranes from nontransfected HEK293 cells (data not shown). The affinity of [^{125}I]NDP-MSH was similar for WT and mutant receptors (Table 1) suggesting that these mutations did not dramatically alter receptor structure. The level of functional receptor expression (B_{max}) was also similar for WT and mutant receptors (0.72−2.0 pmol/mg, Table 1), with the exception of M200A for which the level was lower (0.17 pmol/mg).

Binding affinity of the endogenous peptide agonist α-MSH was reduced by D122A, M200A, F261A, and F284A mutations, in agreement with previous studies (*28*−*30*), but was unaffected by S190A and S191A mutations (Figure 2A, Tables 2 and 3). The affinity of five nonpeptide ligands was reduced by D122A mutation (Figure 2, Table 2); affinity of four compounds was affected by M200A (Table 3); affinity of all compounds was reduced by F261A (Figure 2, Table 3); affinity of two compounds was reduced by F284A (Figure 2, Table 3); and affinity was unaffected by S191A (Table 2). These findings indicate that the MC4 receptor binding determinants for nonpeptide ligands overlap those for α-MSH. However, one mutation that did not affect α-MSH affinity reduced binding of nonpeptide ligands: S190A mutation slightly but significantly reduced binding affinity of all nonpeptide ligands tested (Table 2). This result suggests that there might be additional binding determinants for nonpeptide ligands that are not involved in α-MSH binding. AgRP(83−132) affinity was reduced by only two of the mutations that affected nonpeptide ligand binding (F261A and F284A, Figure 2B, Table 3, consistent with previous studies (*28*−*32*)), suggesting less overlap between the binding determinants for this endogenous antagonist peptide and those for nonpeptide ligands. By contrast, affinity of MBP10, a small synthetic cyclic peptide antagonist, was reduced by all five of the mutations that affected binding of one or more nonpeptide ligand (D122A, S190A, M200A, F261A, and F284A, Figure 2C, Tables 2 and 3). This finding indicates substantial overlap between the binding determinants of this peptide antagonist and those for nonpeptide ligands.

Role of Hydrophobic Residues in TM6 and TM7 in Nonpeptide Ligand Interaction. We next examined the mechanism by which TM6/TM7 mutations affected nonpeptide ligand binding by comparing effects of receptor mutation on binding of functionally and structurally distinct nonpeptide ligands. As described above, two aromatic residues were identified that acted as determinants of nonpeptide ligand binding to the MC4 receptor: F261 in TM6 and F284 in TM7. The effect of these mutations was first compared for nonpeptide ligands of varying efficacy for stimulation of cAMP accumulation (Figure 1B−D), to examine the extent to which the mutations' effects correlated with ligand efficacy. Ligands tested were the full agonist piperazine-1, the partial agonists piperazines-2 and -3, and the antagonists piperazine-4, piperazine-5, and benzamidine-1 (Figure 1B−D). A clear relationship was observed between ligand efficacy and sensitivity to F261A and F284A mutations. F284A mutation reduced affinity of the antagonists piperazine-4, piperazine-5, and benzamidine-1 (5.5-, 6.6-, and 7.5-fold, respectively) but did not significantly affect the affinity of the partial agonists (piperazine-2 and piperazine-3) or the agonist (piperazine-1) (Figure 2, Table 3). F261A mutation reduced affinity of antagonists piperazine-4, piperazine-5, and benzamidine-1 by 67-, 48-, and 46-fold, respectively; reduced affinity of partial agonists piperazine-2 and piperazine-3 to a slightly smaller extent (26- and 31-fold, respectively); and reduced affinity of the full agonist piperazine-1 by only 13-fold (Figure 2, Table 3). Overall, these findings indicate the lower the signaling efficacy of the ligand, the greater the affinity-reducing effect of F261A and F284A mutations.

We next attempted to correlate the effect of F261A and F284A mutations with nonpeptide ligand structure to identify the ligand determinant underlying sensitivity to the mutations. F261A mutation reduced binding affinity of all compounds tested, suggesting that the ligand determinant underlying this effect is common to all the compounds. The most obvious common determinant is the halogenated phenyl group (Figure 1B−D; 4-chlorophenyl for piperazines-1−3; 2,4-dichlorophenyl for piperazine-4 and piperazine-5; and either the 2-fluorophenyl or 5-bromo-2-methoxyphenyl groups of benzamidine-1). The substituents on the phenyl group of the piperazine series of compounds determined the magnitude of the mutations' effect: F284A mutation reduced affinity of 2,4-dichlorophenyl compounds (5.5-fold for piperazine-4 and 6.6-fold for piperazine-5) but did not significantly affect the affinity of 4-chlorophenyl compounds (piperazines-1−3), Figure 2, Table 3). F261A mutation had a slightly greater affinity-reducing effect on 2,4-dichlorophenyl compounds (67- and 48-fold for piperazine-4 and piperazine-5, respectively) than on 4-chlorophenyl compounds (13-, 26-, and 31-fold for piperazine-1, piperazine-2, and piperazine-3, respectively, Figure 2, Table 3). F284A mutation also eliminated the affinity-enhancing effect of the additional chlorine at the 2-position. Specifically, piperazine-4 bound the WT receptor with 6.1-fold higher affinity than piperazine-3 (Figure 2F,G, Table 3), the only difference

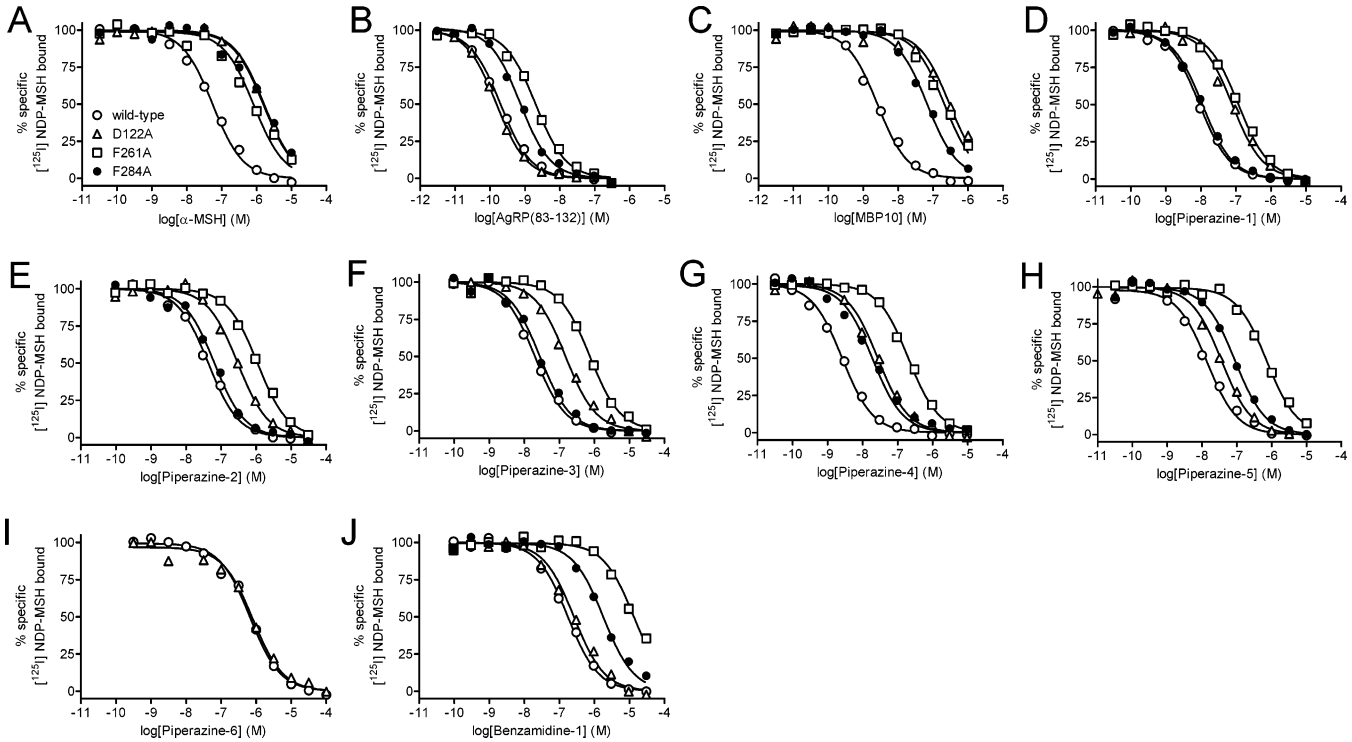

FIGURE 2: Effect of MC4 receptor mutations on binding of peptide and nonpeptide ligands. Binding of unlabeled ligands was measured by displacement of [^{125}I]NDP-MSH binding to membranes from HEK293 cells expressing wild-type, D122A, F261A, and F284A mutant MC4 receptors, as described in Experimental Procedures. (S190A, S191A, and M200A mutants were also tested, but the data have been omitted for clarity since their effect on ligand binding was slight; binding data for all mutations is given in Tables 2 and 3.) Ligands tested were the peptide agonist α-MSH (A); the peptide antagonist AgRP(83−132) (B); the small cyclic peptide antagonist MBP10 (C); the nonpeptide agonist piperazine-1 (D); the nonpeptide partial agonists piperazine-2 (E) and piperazine-3 (F); and the nonpeptide antagonists piperazine-4 (G), piperazine-5 (H), piperazine-6 (I), and benzamidine-1 (J). (See Figure 1B−D for ligand structures.) Piperazine-6 was tested on WT and D122A mutant receptors only. Data points are single determinations. Data are from representative experiments performed three times with similar results, except piperazine-6 ($n = 5$).

Table 2: Affinity of Peptide and Nonpeptide Ligands for Wild-Type and Mutant MC4 Receptors (Transmembrane Domain 3 and Extracellular Loop 2 Mutations)[a]

	wild-type	D122A		S190A		S191A	
ligand	pK_i **K_i, nM**	pK_i **K_i, nM**	fold-shift	pK_i **K_i, nM**	fold-shift	pK_i **K_i, nM**	fold-shift
α-MSH	7.37 ± 0.04	5.88 ± 0.13[b]	31	7.19 ± 0.04	1.5	7.45 ± 0.05	0.82
(agonist)	**43**	**1300**		**65**		**36**	
AgRP(83−132)	9.88 ± 0.04	10.0 ± 0.04	0.77	9.69 ± 0.04	1.6	9.91 ± 0.01	0.95
(antagonist)	**0.13**	**0.10**		**0.21**		**0.12**	
MBP10	8.63 ± 0.08	6.67 ± 0.04[b]	92	8.18 ± 0.06[b]	2.8	8.61 ± 0.02	1.1
(antagonist)	**2.3**	**212**		**6.6**		**2.5**	
piperazine-1	8.24 ± 0.02	7.29 ± 0.02[b]	8.8	7.96 ± 0.04[d]	1.9	8.35 ± 0.02	0.77
(agonist)	**5.8**	**51**		**11**		**4.4**	
piperazine-2	7.40 ± 0.07	6.72 ± 0.03[b]	4.7	7.06 ± 0.03[b]	2.2	7.44 ± 0.01	0.92
(partial agonist)	**40**	**190**		**88**		**36**	
piperazine-3	7.86 ± 0.02	7.08 ± 0.03[b]	5.9	7.54 ± 0.05[c]	2.1	7.88 ± 0.06	0.94
(partial agonist)	**14**	**83**		**29**		**13**	
piperazine-4	8.63 ± 0.07	7.75 ± 0.05[b]	7.7	8.16 ± 0.06[b]	3.0	8.54 ± 0.06	1.3
(antagonist)	**2.3**	**18**		**6.9**		**2.9**	
piperazine-5	8.05 ± 0.06	7.44 ± 0.01[b]	4.1	7.69 ± 0.07[b]	2.3	8.06 ± 0.07	0.99
(antagonist)	**8.9**	**37**		**20**		**8.8**	
benzamidine-1	6.89 ± 0.04	6.82 ± 0.02	1.2	6.53 ± 0.03[b]	2.3	6.91 ± 0.04	0.96
(antagonist)	**130**	**150**		**300**		**120**	

[a] Ligand affinity was measured by inhibition of [^{125}I]NDP-MSH binding to membranes from HEK293 cells expressing wild-type and mutant receptors, as described in Experimental Procedures. See Figure 1B−D for ligand structures. The IC_{50} for inhibition of radioligand binding was converted to K_i using the Cheng-Prusoff equation (*54*), using values of K_d from [^{125}I]NDP-MSH saturation experiments (see Table 1). For each ligand, pK_i for all mutants (in Tables 2 and 3) was statistically compared with the value for wild-type ([b]$p < 0.001$, [c]$p < 0.01$, [d]$p < 0.05$, two-factor ANOVA followed by Bonferroni post-test comparing wild-type with each of the six mutant receptors). This analysis was used to determine whether each mutation affected ligand affinity relative to the wild-type receptor. Data are mean ± SEM ($n = 3$).

between the compounds being the additional 2-chloro substituent of the former (Figure 1C). At the F284A mutant receptor the difference of affinity was reduced to 1.5-fold (Figure 2F,G, Table 3). Taken together, all these findings indicate the halogenated phenyl group is a determinant of the F261A and F284A mutations' affinity-reducing effect.

Table 3: Affinity of Peptide and Nonpeptide Ligands for Wild-Type and Mutant MC4 Receptors (Transmembrane Domain 5, 6 and 7 Mutations)[a]

	wild-type	M200A		F261A		F284A	
ligand	pK_i **K_i, nM**	pK_i **K_i, nM**	fold-shift	pK_i **K_i, nM**	fold-shift	pK_i **K_i, nM**	fold-shift
α-MSH (agonist)	7.37 ± 0.04 **43**	6.97 ± 0.03[b] **110**	2.5	6.56 ± 0.07[b] **270**	6.3	6.22 ± 0.06[b] **600**	14
AgRP(83−132) (antagonist)	9.88 ± 0.04 **0.13**	10.1 ± 0.08 **0.084**	0.64	8.94 ± 0.07[b] **1.2**	8.9	9.35 ± 0.05[b] **0.45**	3.4
MBP10 (antagonist)	8.63 ± 0.08 **2.3**	8.19 ± 0.08[b] **6.5**	2.8	6.77 ± 0.12[b] **170**	73	7.32 ± 0.06[b] **48**	21
piperazine-1 (agonist)	8.24 ± 0.02 **5.8**	7.50 ± 0.07[b] **31**	5.4	7.14 ± 0.06[b] **73**	13	8.11 ± 0.02 **7.7**	1.3
piperazine-2 (partial agonist)	7.40 ± 0.07 **40**	7.06 ± 0.05[c] **87**	2.2	5.98 ± 0.08[b] **1000**	26	7.39 ± 0.03 **41**	1.0
piperazine-3 (partial agonist)	7.86 ± 0.02 **14**	7.46 ± 0.05[b] **35**	2.5	6.37 ± 0.05[b] **430**	31	7.69 ± 0.01 **20**	1.5
piperazine-4 (antagonist)	8.63 ± 0.07 **2.3**	8.40 ± 0.01 **4.0**	1.7	6.81 ± 0.01[b] **160**	67	7.89 ± 0.03[b] **13**	5.5
piperazine-5 (antagonist)	8.05 ± 0.06 **8.9**	8.09 ± 0.24 **8.2**	0.92	6.37 ± 0.03[b] **430**	48	7.24 ± 0.01[b] **58**	6.6
benzamidine-1 (antagonist)	6.89 ± 0.04 **130**	7.14 ± 0.07[d] **72**	0.56	5.23 ± 0.02[b] **5900**	46	6.02 ± 0.08[b] **960**	7.5

[a] See legend to Table 2 for further details and Figure 1B−D for ligand structures. For each ligand, pK_i for all mutants in Tables 2 and 3 was statistically compared with the value for wild-type ([b]$p < 0.001$, [c]$p < 0.01$, [d]$p < 0.05$, two-factor ANOVA followed by Bonferroni post-test comparing wild-type with each of the six mutant receptors). This analysis was used to determine whether each mutation affected ligand affinity relative to the wild-type receptor. Data are mean ± SEM ($n = 3$).

Table 4: Ligand Potency and Efficacy for Stimulating cAMP Accumulation via Wild-Type and Mutant MC4 Receptors[a]

	wild-type		D126A			F261A			F284A		
ligand	pEC_{50} **EC_{50}, nM**	E_{max} (%)	pEC_{50} **EC_{50}, nM**	fold shift	E_{max} (%)	pEC_{50} **EC_{50}, nM**	fold shift	E_{max} (%)	pEC_{50} **EC_{50}, nM**	fold shift	E_{max} (%)
NDP-MSH	9.30 ± 0.06 **0.50**	100	6.17 ± 0.07 **670**[b]	1400	100	9.20 ± 0.07 **0.63**	1.3	100	9.26 ± 0.17 **0.56**	1.1	100
piperazine-1	8.70 ± 0.07 **2.0**	94 ± 11	5.18 ± 0.15 **6600**[b]	3300	62 ± 7	7.33 ± 0.10 **46**[b]	23	120 ± 20	8.41 ± 0.09 **3.9**	1.9	120 ± 19
THIQ	9.31 ± 0.05 **0.49**	102 ± 9	6.57 ± 0.05 **270**	550	75 ± 2						
piperazine-2	6.82 ± 0.09 **150**	21 ± 4				5.91 ± 0.06 **1200**	8.1	46 ± 2[c]			
piperazine-3	7.72 ± 0.14 **19**	28 ± 5				6.52 ± 0.05 **300**	16	63 ± 2[d]			
piperazine-4	NA[e]	2[e]				6.20 ± 0.14 **630**	NA[e]	23 ± 1[c]			

[a] Accumulation of cAMP was measured for the receptors expressed in HEK293 cells as described in Experimental Procedures. See Figure 1B,C for ligand structures. Agonist concentration−response curves were fitted to a four-parameter logistic equation to obtain fitted values of pEC_{50} (−logEC_{50}) and E_{max}. The EC_{50} shift for the mutant receptors was calculated by dividing the mean EC_{50} for the mutant receptor by the mean EC_{50} for the wild-type receptor. The %E_{max} was calculated by dividing the agonist-specific cAMP accumulation by that for NDP-MSH. The NDP-MSH E_{max} for stimulating cAMP accumulation for wild-type, D126A, F261A, and F284A receptors was 28 ± 2, 14 ± 3, 28 ± 3, and 25 ± 4 pmol of cAMP/10^4 cells, respectively. The value for D126A was significantly different from wild-type ($p < 0.05$, single-factor ANOVA followed by Dunnett's Multiple Comparison Test comparing mutant receptors with wild-type). cAMP accumulation in the absence of agonist varied between 0.1 and 1.1 pmol of cAMP/10^4 cells. The slope factor from the four-parameter logistic equation fits was between 0.7 and 1.4. The slope was fixed at unity for the partial agonist ligands. Differences of EC_{50} of NDP-MSH and piperazine-1 between mutant and wild-type receptors was tested statistically by two-factor ANOVA, followed by Bonferroni post-test comparing wild-type with each of the three mutant receptors. [b] $p < 0.001$. Differences of piperazine ligand E_{max} between wild-type and F261A receptors were tested statistically by two-factor ANOVA followed by Bonferroni post-test comparing wild-type with F261A: [c] $p < 0.01$. [d] $p < 0.001$. [e] Due to the very low intrinsic activity for piperazine-4 at the wild-type receptor a four-parameter logistic equation could not be reliably fitted to the data, so the %E_{max} was calculated for the response at 10 μM compound. Data are mean ± SEM from 3 to 10 independent experiments.

The effect of the F261A and F284A mutations was next evaluated in functional assays (stimulation of cAMP accumulation), to evaluate the mutations' effects on ligand efficacy (E_{max}), and to compare the mutations' effect on functional potency (EC_{50}) with the effect on MC4 receptor binding affinity (K_i). We first evaluated peptide agonists. α-MSH and NDP-MSH stimulated cAMP accumulation in HEK293 cells expressing WT, F261A, and F284A receptors (Figures 3−5, Table 4). The efficacy of α-MSH and NDP-MSH was not significantly different between WT and mutant receptors (legend to Figure 3 for α-MSH; Table 4 for NDP-MSH). The potency of NDP-MSH was also not significantly different between WT and the two mutant receptors (Table 4). These results support the hypothesis that F261A and F284A mutations do not dramatically alter receptor structure. The potency of α-MSH was significantly reduced by F261A and F284A mutations (12- and 11-fold, respectively; see legend to Figure 3). These reductions are similar to the effects on MC4 receptor binding affinity (6.3- and 14- fold decrease of affinity, respectively, Table 3), validating the binding data.

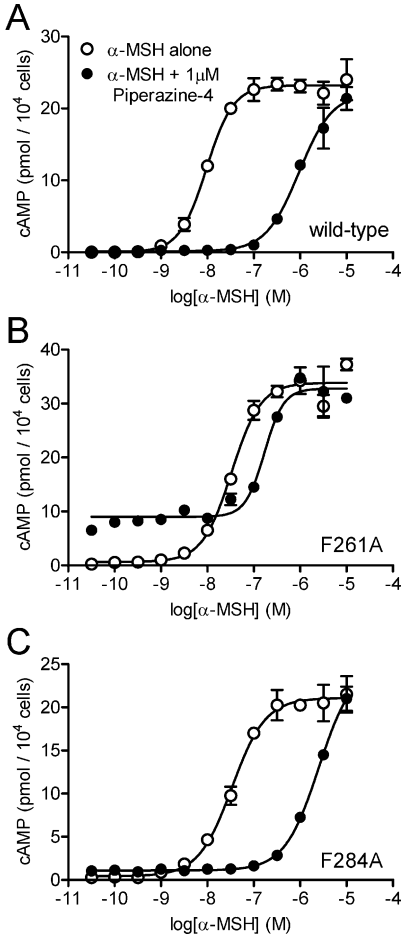

FIGURE 3: Antagonist activity of piperazine-4 on α-MSH-stimulated cAMP accumulation. Antagonist activity was measured by determining the effect of 1 μM piperazine-4 (Figure 1C) on the α-MSH dose−response for stimulation of cAMP accumulation in HEK293 cells expressing wild-type (A), F261A (B), and F284A (C) MC4 receptors, as described in Experimental Procedures. The curves are fits to a four-parameter logistic equation, and data points are mean ± range of duplicate determinations (where range is standard deviation divided by the square-root of *n*). Data are from representative experiments performed 4−6 times with similar results. Note that the basal response at the F261A MC4 receptor is higher in the presence of piperazine-4 than in the absence of the nonpeptide ligand, suggesting that the mutation introduces agonist activity of the compound (also see Figure 4). pK_b values for the antagonist were determined from the extent of shift of the α-MSH EC_{50}, as described in Experimental Procedures, Data Analysis. The derived pK_b value for Piperazine-4 for wild-type, F261A, and F284A was 7.85 ± 0.23, 6.28 ± 0.14, and 7.05 ± 0.17 respectively (mean ± SEM, $n = 4-6$, with corresponding K_b values of 14, 520, and 89 nM). Single factor ANOVA indicated a significant difference between pK_b values for the different receptors, with Dunnett's multiple comparison test, comparing mutants with wild-type, indicating the value for F261A and F284A differed significantly from the value for wild-type ($p < 0.01$ and $p < 0.05$ respectively). α-MSH stimulated cAMP accumulation via wild-type, F261A, and F284A receptors with $-\log EC_{50}$ values of 8.05 ± 0.18, 6.97 ± 0.26, and 7.02 ± 0.18, respectively (corresponding EC_{50} values of 8.9, 110, and 95 nM). Single factor ANOVA followed by Dunnett's multiple comparison test indicated $-\log EC_{50}$ for F261A and F284A was significantly different from wild-type ($p < 0.01$). The α-MSH E_{max} for wild-type, F261A, and F284A receptors was 20 ± 4, 19 ± 6, and 21 ± 5 pmol/10 000 cells, respectively. These values are not significantly different ($p = 0.97$, single-factor ANOVA).

The functional effect of F261A and F284A mutations was then evaluated for nonpeptide ligands. The nonpeptide agonist piperazine-1 was a potent full agonist on the WT MC4 receptor (EC_{50} of 2.0 nM, E_{max} 94% of the NDP-MSH E_{max}, Table 4). The F261A and F284A mutations did not affect efficacy of the compound (Table 4, Figure 5B for F261A). However, F261A mutation reduced potency of piperazine-1 by 23-fold (Figure 5B, Table 4), in approximate agreement with the reduction of receptor binding affinity (13-fold, Figure 2D, Table 3). F284A mutation did not significantly affect potency of piperazine-1 (Table 4), in agreement with the receptor binding data (Figure 2D, Table 3).

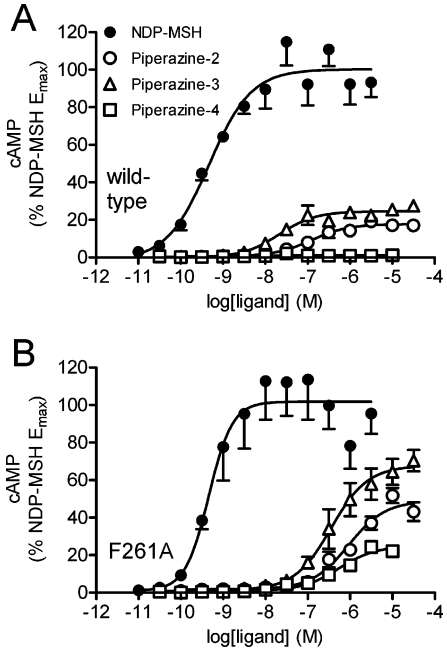

FIGURE 4: Effect of F261A mutation on stimulation of cAMP accumulation by nonpeptide partial agonist and antagonist ligands. Accumulation of cAMP in HEK293 cells expressing wild-type (A) or F261A (B) MC4 receptors was measured as described in Experimental Procedures. The nonpeptide ligands tested were the partial agonists piperazine-2 and piperazine-3, and the nonpeptide antagonist piperazine-4. (See Figure 1C for ligand structures.) The curves are fits to a four-parameter logistic equation, and data points are mean ± range of duplicate determinations (where range is the standard deviation divided by the square-root of *n*). Data are from representative experiments performed three times with similar results.

Whole cell cAMP accumulation assays were then used to assess the antagonist potency (K_b) of piperazine-4. Antagonist potency was measured by quantifying the effect of the compound on the α-MSH EC_{50} for stimulation of cAMP accumulation (Figure 3). The extent of the shift of EC_{50} was used to calculate the K_b of piperazine-4 (concentration of antagonist required to double the α-MSH EC_{50}; see Experimental Procedures, Data Analysis). The K_b of piperazine-4 for the WT receptor was 14 nM (Figure 3A). The K_b was significantly increased by F261A and F284A mutations (37- and 6.3-fold, Figure 3B,C). These reductions of functional antagonist potency are similar to the reductions of piperazine-4 binding affinity (67- and 5.5-fold reduction for F261A and F284A mutations, respectively, Table 3), validating the binding data.

On measuring the antagonist potency of piperazine-4, it was apparent that the presence of the compound (1 μM) elevated the level of cAMP via the F261A mutant (Figure 3B) but did not appreciably affect cAMP via the WT MC4 receptor (Figure 3A). This finding suggests that F261A

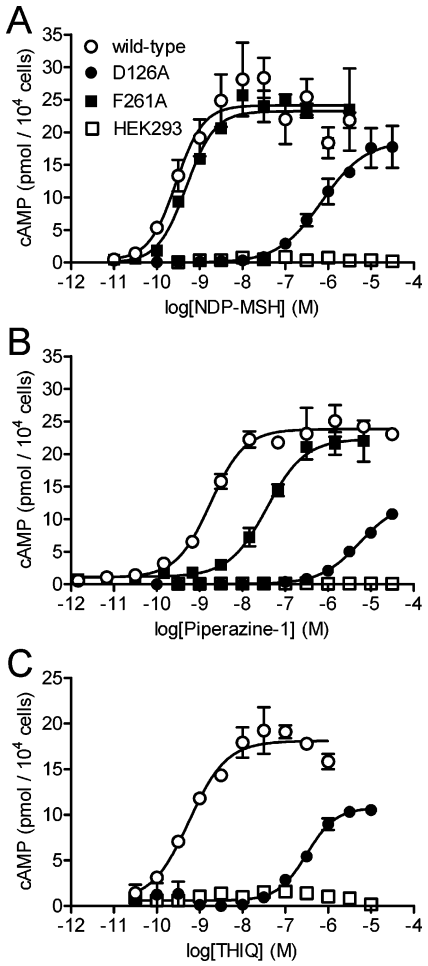

FIGURE 5: Effect of D126A and F261A mutations on stimulation of cAMP accumulation by agonist ligands. Accumulation of cAMP in parental HEK293 cells, or cells expressing wild-type or mutant MC4 receptors, was measured as described in Experimental Procedures, for the peptide agonist NDP-MSH (A), and the nonpeptide agonists piperazine-1 (B) and THIQ (C). (See Figure 1B for ligand structures.) The curves are fits to a four-parameter logistic equation, and data points are mean ± range of duplicate determinations (where range is standard deviation divided by the square-root of *n*). Data are from representative experiments performed 3−10 times with similar results.

mutation introduced detectable receptor activation by piperazine-4. The effect of this mutation on ligand-stimulated cAMP accumulation was further evaluated by measuring the dose−response for cAMP accumulation stimulated by piperazine-4. We also tested the effect of the mutation on the dose−response for the partial agonists piperazine-2 and piperazine-3. On the WT receptor the E_{max} of piperazine-1, piperazine-2, and piperazine-3 was 2, 21, and 28% of the NDP-MSH E_{max}, respectively (Figure 4A, Table 4). On the F261A receptor, piperazine-4 detectably stimulated cAMP accumulation via the F261A receptor (E_{max} of 23%, Figure 4B, Table 4). In addition, the E_{max} of piperazine-2 and piperazine-3 on the F261A mutant (46 and 63%, respectively, Figure 4B, Table 4) was significantly increased relative to the WT receptor (21 and 28%, respectively, Figure 4A, Table 4). These findings indicate that F261A mutation increased efficacy of the nonpeptide antagonist and partial agonist ligands tested.

Effect of S190A and M200A Mutations on Ligand Affinity. S190A mutation in extracellular loop 2 (Figure 1A) slightly but significantly reduced affinity of all nonpeptide ligands tested (1.9−3.0-fold) and also slightly reduced affinity of MBP10 (2.8-fold). No ligand-specific effects were observed with this mutation. M200A mutation in TM5 (Figure 1A) affected binding of certain nonpeptide ligands and MBP10 (Table 3). The largest reduction of affinity was for the agonist piperazine-1 (5.4-fold), with smaller reductions observed for piperazine partial agonists and antagonists (Table 3). M200A mutation slightly increased (1.8-fold) affinity of benzamidine-1 (Table 3).

Role of TM3 Acidic Residues in Nonpeptide Ligand Interaction. Two acidic residues in TM3 of the MC4 receptor (D122 and D126) have been shown to be involved in peptide ligand binding (*28*−*30*, *32*, see also Table 2). With respect to nonpeptide ligands, D122A mutation reduced affinity of piperazines 1−5 to a similar extent (4.1−8.8-fold) but did not affect binding of benzamidine-1 (Figure 2, Table 2). This finding suggests that a common determinant of piperazines 1−5 was responsible for the affinity-reducing effect of D122A mutation. The identity of this determinant was investigated. Some of the molecular modeling and peptide/nonpeptide superposition results suggests the "right-hand-side" of the ligand, as drawn in Figure 1, interacts with an acidic pocket of the MC4 receptor that includes D122 (*40*, *50*). This hypothesis was tested using a compound that lacks the derivatized amide functionality of piperazines-2 and -3 (piperazine-6). Piperazine-6 bound the WT MC4 receptor with a pK_i of 6.18 ± 0.10 ($n = 5$, $K_i = 660$ nM, Figure 2I). The ligand bound the D122A mutant receptor with a pK_i of 6.33 ± 0.10 ($n = 5$, $K_i = 470$ nM, Figure 2I), a value not significantly different from that for the WT receptor ($p = 0.87$, two-tailed Student's t-test). This finding indicates the "right-hand side" region of the piperazine compounds is a determinant of the affinity-reducing effect of D122A mutation.

We next examined the effect of D126A mutation on ligand interaction. Ligand-stimulated cAMP accumulation was used for this purpose since D126A mutation eliminated detectable binding of [^{125}I]NDP-MSH and [^{125}I]AgRP(83−132). We first evaluated the effect of D126A mutation on peptide agonist potency (EC_{50}) and efficacy (E_{max}). NDP-MSH stimulated cAMP accumulation via the D126A mutant receptor in a dose-dependent manner (Figure 5A). However, the mutation dramatically reduced potency (1400-fold, from an EC_{50} of 0.5 nM for the WT MC4 receptor to 670 nM for the mutant receptor, Figure 5A, Table 4). The mutation also reduced the total level of cAMP accumulation stimulated by NDP-MSH (from 28 pmol/10^4 cells for WT to 14 pmol/10^4 cells for D126A receptors, Table 4). α-MSH did not appreciably stimulate cAMP accumulation via the D126A mutant receptor at concentrations up to 30 μM (data not shown). These data indicate that D126A mutation substantially reduced peptide agonist interaction with the MC4 receptor, consistent with the findings of previous studies (*28*, *29*).

The effect of D126A mutation on nonpeptide agonist interaction was evaluated next. D126A mutation dramatically reduced the potency of the nonpeptide agonist piperazine-1 (3300-fold, from an EC_{50} of 2.0 nM for the WT receptor to 6.6 μM for the D126A mutant, Figure 5B, Table 4). Similarly, D126A mutation strongly reduced the potency of a different nonpeptide agonist THIQ (550-fold, Figure 5C,

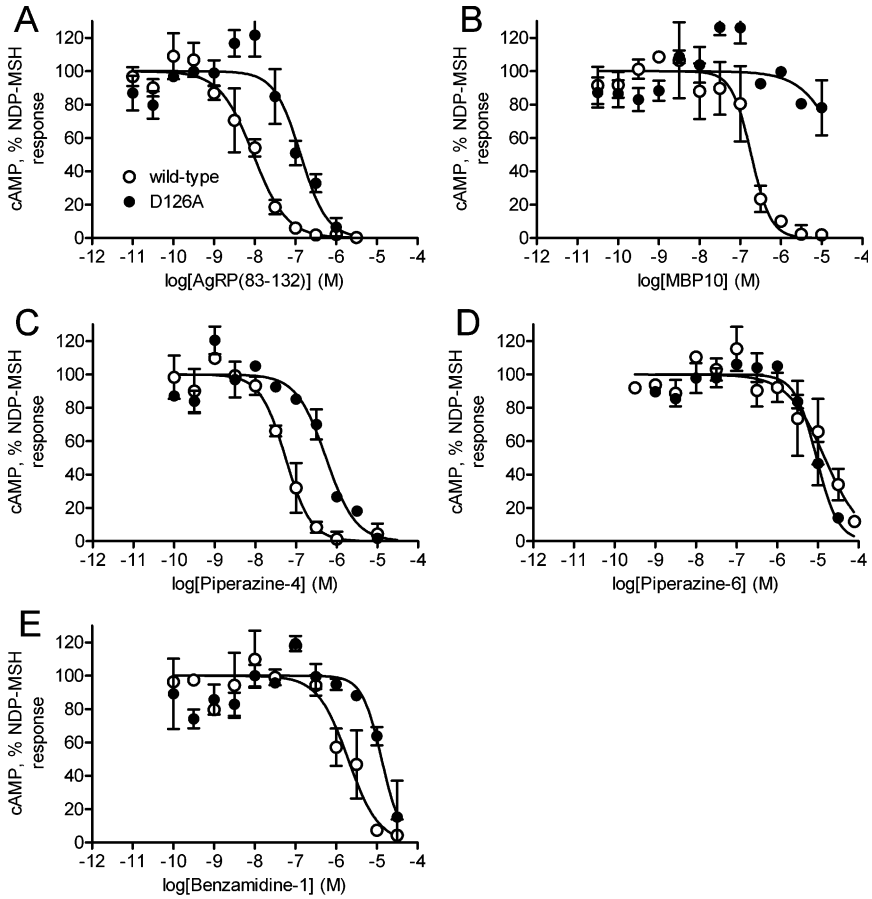

FIGURE 6: Effect of D126A mutation on antagonist interaction with the MC4 receptor. Antagonist interaction with wild-type and D126A mutant receptors was measured by antagonism of cAMP accumulation stimulated by NDP-MSH, as described in Experimental Procedures. The ratio of NDP-MSH concentration used vs EC_{50} was approximately equal for both wild-type and D126A receptors (1 vs 0.5 nM for wild-type, and 1 μM vs 650 nM for D126A). The ligands tested were AgRP(83−132) (A), MBP10 (B), piperazine-4 (C), piperazine-6 (D), benzamidine-1 (E), piperazine-2, piperazine-3, and piperazine-5 (graphical data not shown). (See Figure 1C,D for ligand structures.) The curves are fits to a four-parameter logistic equation, and data points are mean ± range of duplicate determinations (where range is standard deviation divided by the square-root of *n*). Data are from representative experiments performed 3−8 times with similar results.

Table 4). These data indicate that the D126A mutation strongly reduces nonpeptide agonist interaction with the MC4 receptor. The mutation also slightly reduced the E_{max} of nonpeptide agonists, relative to NDP-MSH: At the WT receptor, piperazine-1 and THIQ were full agonists (94 and 102% of the NDP-MSH E_{max}, respectively, Table 4), whereas at D126A the compounds were partial agonists (62 and 75%, respectively, Table 4). This result implies that the D126A mutation slightly impairs, but does not eliminate, the signaling efficacy of nonpeptide agonists on the MC4 receptor.

We next tested the effect of D126A mutation on antagonist ligand interaction, to compare the effect of the mutation on agonist versus antagonist receptor interaction. Antagonist potency (IC_{50}) was measured by inhibition of the cAMP response produced by NDP-MSH. Concentrations of NDP-MSH were used for WT and D126A receptors (1 nM and 1 μM, respectively) that were close to the NDP-MSH EC_{50} for each receptor (0.5 and 670 nM, respectively, Table 4), enabling meaningful comparison of antagonist IC_{50}. Potency of nonpeptide antagonists was reduced by D126A mutation to a similar extent [13-fold for piperazine-2, 6.1-fold for piperazine-3, 11-fold for piperazine-4 (Figure 6C), 12-fold for piperazine-5, and 17-fold for benzamidine-1 (Figure 6E), see Table 5]. The magnitude of these effects on nonpeptide antagonist IC_{50} was much less than the effect on nonpeptide agonist EC_{50} (550−3300-fold, Table 4).

The determinant of the piperazine antagonist ligand underlying sensitivity to the D126A mutation was investigated. As described above, some studies have suggested that the right-hand side of the compounds interacts with an acidic pocket of the MC4 receptor that includes D126A (*40*, *50*). The role of the right-hand side of piperazine ligands in mediating sensitivity to D126A mutation was tested using piperazine-6, a ligand that lacks this region (Figure 1C). This compound antagonized NDP-MSH-stimulated cAMP accumulation via both WT and D126A receptors (Figure 6D). The potency for this effect was not significantly different between WT and D126A mutant receptors (Table 5). This finding indicates that the right-hand side of piperazine ligand is a determinant of the potency-reducing effect of the D126A mutation.

DISCUSSION

The aims of this study were to identify amino acids of the MC4 receptor that acted as determinants of nonpeptide ligand binding; to identify molecular interactions between nonpeptide ligands and the receptor; and to compare receptor interactions of nonpeptide agonists versus antagonists. The principal findings are the following: (i) Nonpeptide ligand affinity was affected by D122A, D126A, S190A, M200A, F261A, and F284A mutations; (ii) The halogenated aromatic group of nonpeptide ligand was a determinant of sensitivity

Table 5: Ligand Potency for Antagonizing NDP-MSH-Stimulated cAMP Accumulation via Wild-Type and D126A Mutant MC4 Receptors[a]

	pIC_{50} **IC_{50}, nM**		
antagonist	wild-type	D126A	fold shift
AgRP(83−132)	8.26 ± 0.23 **5.5**	6.99 ± 0.12[b] **100**	19
MBP10	6.95 ± 0.20 **110**	<5	>90
piperazine-2	6.27 ± 0.25 **540**	5.15 ± 0.28[c] **7100**	13
piperazine-3	6.85 ± 0.33 **140**	6.06 ± 0.04[b] **870**	6.1
piperazine-4	7.55 ± 0.12 **28**	6.62 ± 0.16[b] **240**	8.5
piperazine-5	7.57 ± 0.16 **27**	6.51 ± 0.06[b] **310**	12
piperazine-6	4.89 ± 0.17 **13000**	4.91 ± 0.09 **12000**	0.95
benzamidine-1	5.89 ± 0.17 **1300**	4.66 ± 0.12[b] **22000**	17

[a] Antagonist activity was measured by inhibition of NDP-MSH-stimulated cAMP accumulation in HEK293 cells expressing wild-type and D126A MC4 receptors (see Experimental Procedures). Antagonist pIC_{50} ($-\log IC_{50}$) was determined by fitting inhibition data to a four-parameter logistic equation. (The slope factor in these fits was between 0.9 and 1.7). The concentration of NDP-MSH used (1 nM for wild-type and 1 μM for D126A) was approximately double the NDP-MSH EC_{50} for both receptors (0.5 nM for wild-type and 670 nM for D126A). See Figure 1C,D for ligand structures. For each ligand pIC_{50} for the D126A receptor was statistically compared with the value for wild-type ([b]$p < 0.001$; [c]$p < 0.01$; two-factor ANOVA followed by Bonferroni post-test). MBP10 was not included in this analysis because the antagonism on the D126A receptor was too weak to accurately determine an IC_{50} value. Data are mean ± SEM, $n = 3-8$.

to F261A and F284A mutations; (iii) The "right-hand side" of piperazine ligands was a determinant of sensitivity to D122A and D126A mutations; (iv) Sensitivity to F261A and F284A mutation was correlated with ligand efficacy − antagonist affinity was reduced more strongly than partial agonist and agonist affinity. (v) F261A mutation increased efficacy of nonpeptide partial agonist and antagonist ligands. These findings imply a binding orientation in which the ligands' halogenated aromatic group binds F261/F284, and the right-hand side binds in the vicinity of D122 and D126. Moreover, the strength of the F261/F284 interaction controls receptor activation, in that the stronger the interaction with these residues, the lower the ligand's efficacy.

We first compared molecular determinants of peptide and nonpeptide ligand binding to the MC4 receptor. With respect to agonists, piperazine agonist affinity was reduced by four mutations which reduced binding of α-MSH (D122A, D126A, M200A, and F261A, Tables 2−4, see also refs *28*−*30* for α-MSH). These results imply piperazine agonists and α-MSH occupy an overlapping space when bound to the receptor. However, piperazine agonist affinity was reduced by one mutation that did not affect binding of α-MSH (S190A), and reciprocally α-MSH affinity was reduced by a mutation that did not affect binding of piperazine agonists (F284A), implying the binding sites do not completely overlap. With respect to antagonists, there was complete overlap between the mutations that reduced binding of piperazine antagonists (piperazine-4 and -5) and MPB10 (a small cyclic peptide) (D122A, D126A, S190A, M200A, F261A, and F284A). This finding implies substantial overlap of the receptor space occupied by the piperazine antagonists and MBP10. The binding profile of benzamidine-1, a smaller structurally distinct nonpeptide antagonist, was slightly different from piperazine antagonists. While binding of piperazine and benzamidine antagonists was reduced by D126A, S190, F261A, and F284A mutations, binding affinity of benzamidine-1 was unaffected by D122A and was slightly increased by M200A mutation (Tables 2 and 3). These results suggest partial overlap of the receptor space occupied by piperazine and benzamidine antagonist ligands, especially in the vicinity of F261 and F284.

We next attempted to identify molecular interactions between amino acid side chains of the receptor and functional groups of the ligand, by comparing the effect of mutations between ligands of distinct chemical structure. The findings of this study strongly suggest that the halogenated aromatic group of nonpeptide ligands interacts with F261 and F284. F261A mutation affected binding of all ligands tested, including the structurally distinct benzamidine-1, implying that a common functionality of the compounds underlies the sensitivity to the mutation (Figure 2, Table 3). The only obvious common group is a halogenated aromatic group (Figure 1B−D). For piperazine ligands, the chlorophenyl substitution pattern determined the effect of F261A and F284A mutations. 2,4-Dichloro-substituted compounds were more strongly affected by F261A mutation than 4-chloro-substituted compounds, and only the former were affected by F284A mutation (Table 3). Finally, F284A mutation eliminated the affinity-enhancing effect of the additional 2-chloro-substituent (compare piperazine-3 with piperazine-4, Figure 1C, Table 3). The nature of the interaction between the halogenated aromatic group and the phenyl side chains of F261 and F284 requires further investigation, although π-stacking and/or hydrophobic interactions are likely.

Our findings strongly suggest that the right-hand side of the compounds, as drawn in Figure 1, binds in the vicinity of D122A and D126A. D122A mutation reduced affinity of all piperazine ligands but did not affect binding of benzamidine-1 (Table 2), implying the ligand determinant responsible for the mutation's effect was common and specific to piperazine ligands. Binding of piperazine-6, which lacks the derivatized amide group (the right-hand side) of piperazine-2 and -3, was unaffected by D122A mutation (Figure 2I). The precise interaction between this region of the ligand and D122 requires further evaluation. The magnitude of the mutation's effect (4.1−8.8-fold) is consistent with the loss of a weak hydrogen bond (*56*). Piperazine-6 interaction was also insensitive to D126A mutation, in contrast to all other nonpeptide ligands tested (Tables 4 and 5). The specific interaction between D126 and the right-hand side region can be explored for nonpeptide agonists. D126A mutation strongly reduced potency of piperazine-1 and THIQ (3300- and 550-fold respectively, Figure 4, Table 4), a magnitude consistent with the loss of an electrostatic interaction (*56*). Within the right-hand side region, both piperazine-1 and THIQ bear an amine within the Tic group that could form an electrostatic interaction with the carboxylic acid side chain of D126. The specific interaction between D126 and other nonpeptide ligands remains to be determined. D126A mutation reduced potency of the remaining nonpeptide ligands by 6.1−17-fold (Table 5), a magnitude consistent with the loss of a weak hydrogen bond (*56*).

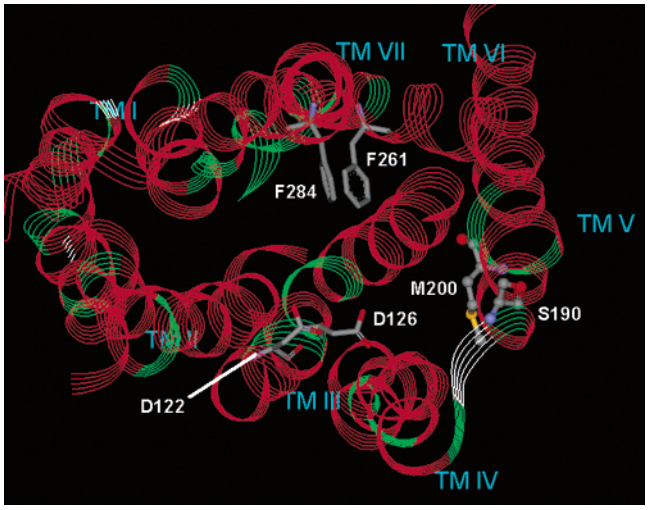

FIGURE 7: Molecular model of the human MC4 receptor identifying determinants of nonpeptide ligand binding. The MC4 receptor was modeled on the X-ray structure of bovine rhodopsin (*57*) as described previously (*39*, *50*). The residues that acted as determinants of nonpeptide ligand interaction, when mutated to alanine, are highlighted ($D122^{3.25}$ and $D126^{3.29}$ in TM3; $S190^{4.66}$ in extracellular loop 2; M200 in TM5; $F261^{6.51}$ in TM6; and $F284^{7.35}$ in TM7). The following have been omitted for clarity: the N-terminal extracellular region, extracellular loops 1 and 3, and all intracellular loops.

Taken together the findings above are consistent with the following binding orientation for piperazine ligands: (i) The chlorophenyl group interacts with the aromatic portions of F261 and F284. (ii) The right-hand side region lies in the vicinity of D122 and D126. This orientation is consistent with one of the previously described molecular models of MC4 receptor−nonpeptide ligand interaction (*39*, *50*). In this homology model utilizing the rhodopsin X-ray structure (*57*), the arrangement of TM helices creates a central cavity that accommodates nonpeptide ligand (*39*, *50*). Figure 7 illustrates the position within this model of residues that are implicated in nonpeptide ligand binding. The phenyl side chains of F261 and F284 are adjacent and project into the binding cavity (Figure 7), such that they could directly interact with the halogenated aromatic group of nonpeptide ligands. F261 and F284 form part of a putative hydrophobic cage of the receptor that can accommodate aromatic groups (*28*, *29*, *50*, *51*). The carboxylic acid side chains of D122 and D126 project toward the binding pocket, consistent with the hypothesis that these residues are directly involved in ligand binding (Figure 7).

A higher resolution, refined molecular model would be useful to evaluate receptor−ligand interactions at an atomic level, but a number of issues require addressing to develop such a model. (i) The structure of TM7 and its spatial arrangement with other transmembrane helices require further investigation. TM7 of rhodpsin is kinked about $P303^{7.50}$ (*57*), within the NPXXY motif that is highly conserved among rhodopsin-like GPCRs (*58*, *59*). $N302^{7.49}$ within the NPXXY sequence of rhodopsin interacts with $D84^{2.50}$ within TM2 (*57*, *59*). The MC4 receptor motif in TM7 is DPLIY (Figure 1A). The N → D substitution in this sequence could alter the kink of TM7 and could alter the arrangement of TM7 and TM2 (which contains the conserved aspartic acid, $D90^{2.50}$, Figure 1A). (ii) Extracellular loop 2 of rhodopsin interacts with TM3 through a highly conserved disulfide bond (*57*, *59*). The MC4 receptor lacks a cysteine in extracellular loop 2 that can form this bond (Figure 1A). This difference could alter the orientation of TM3 of the MC4 receptor with respect to TM4 and 5. (iii) No data are available regarding the structure of receptor-bound nonpeptide ligand, a significant issue considering the size and flexibility of the nonpeptide ligands. These points will require consideration to develop a prospectively useful model. In particular, the arrangement of the hydrophobic cage will need to be quite precisely modeled to orient the halogenated aromatic group, and potentially the whole molecule, within the binding pocket.

The molecular interactions of nonpeptide ligand with the MC4 receptor can be used to assess peptide ligand mimicry, by comparison with the receptor interactions of peptide ligands. Phe^{7} of peptide ligands interacts with residues of the hydrophobic cage (*28*−*30*). The finding that the halogenated aromatic group of nonpeptide ligand binds the same receptor region implies that this group mimics Phe^{7} of peptide ligands. This hypothesis is consistent with peptide/nonpeptide ligand superposition studies (*16*, *40*). Arg^{8} of peptide ligands interacts with D122 and D126, the same region bound by the Tic group amine of nonpeptide agonists. This comparison implies the Tic group amine mimics the charged region of Asp^{8}. This hypothesis is consistent with one of the two ligand superposition studies (*40*). In this superposition, the Tic group amine is oriented close to the basic region of Arg^{8}. Interestingly, the benzene ring of the Tic group is oriented close to the benzene ring of Trp^{9} in this superposition. This aromatic group has been shown to be involved in MC4 receptor activation by nonpeptide agonist (*42*) and peptide agonist (*60*). We speculate that the aromatic group interacts with an unidentified region of the binding pocket to facilitate MC4 receptor activation.

The mechanism of nonpeptide agonist versus antagonist binding to the MC4 receptor was evaluated, by comparing the effect of receptor mutations for ligands of varying efficacy. For F261A and F284A, a clear relationship was evident between affinity reduction and ligand efficacy. Antagonist binding was more strongly reduced than partial and full agonist binding (Figure 2, Table 3). For D126A mutation we were unable to compare ligand affinity directly using radioligand binding assays but were able to measure ligand potency in functional assays (EC_{50} for agonists, IC_{50} for antagonists). Agonist EC_{50} does not provide an unambiguous assessment of agonist affinity owing to the potential for receptor reserve. Two observations suggest little receptor reserve in the expression system used. Increasing expression of the WT receptor did not affect agonist EC_{50} (*30*), implying minimal receptor reserve. NDP-MSH and piperazine-1 binding affinity (0.5 and 5.8 nM, respectively) was similar to functional EC_{50} (0.5 and 2.0 nM, respectively), again implying no great receptor reserve. These considerations suggest that the change of agonist EC_{50} largely reflects a change of binding affinity, an assumption shown to be correct for F261A and F284A mutations where the EC_{50} shift was similar to the binding affinity shift (Tables 2 and 4). D126A mutation more strongly reduced receptor interaction of agonists (550−3300-fold increase of EC_{50}) than antagonists (6.1−17-fold increase of IC_{50}). These data suggest the stronger the ligand interaction with D126A, the higher the signaling efficacy of the ligand. The efficacy-dependent effects of the mutations can be used to propose a thermodynamic model of receptor−ligand interaction and receptor

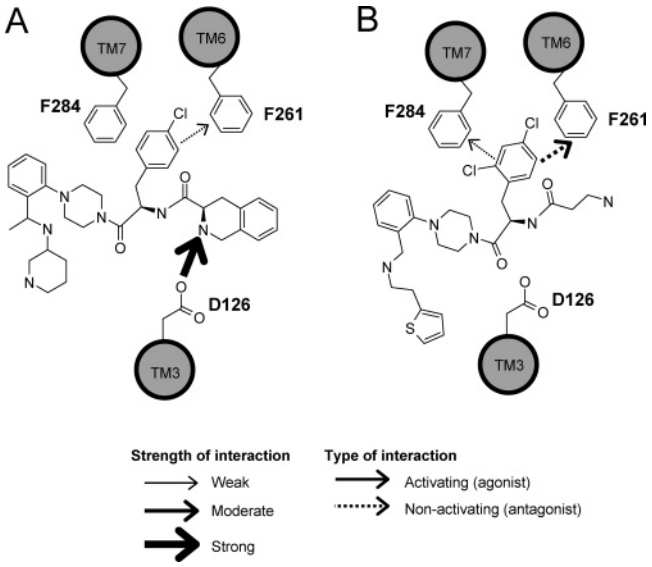

FIGURE 8: Schematic representation of putative MC4 receptor−ligand interactions for a piperazine agonist (A) and a piperazine antagonist (B). Results of this study suggest that the amine of the Tic group of nonpeptide agonists interacts with the carboxylic acid side chain of D126$^{3.29}$ in TM3. The results also suggest that the chlorophenyl group of piperazine ligands interacts with F261$^{6.51}$ and F284$^{7.35}$, residues believed to form part of a putative hydrophobic cage (*28*, *29*, *50*, *51*). The strength of these interactions can be assessed by the reduction of affinity produced by receptor mutation: weak, 2−29-fold reduction of affinity; moderate, 30−300-fold reduction of affinity; strong, >300-fold reduction of affinity. Solid lines indicate receptor−ligand interactions that activate the receptor (promoting agonism), and dashed lines indicate interactions that do not activate the receptor (promoting antagonism). We speculate that antagonist interaction with F261$^{6.51}$ and F284$^{7.35}$ (B) is structurally distinct from agonist interaction with these residues (A), altering the orientation of the nonpeptide ligand within the binding pocket. It is likely that other points of receptor−ligand interaction are involved in nonpeptide ligand binding, beyond those currently identified and illustrated in the figure.

activation (Figure 8). In this model, interaction between the chlorophenyl group and F261/F284 fails to activate the receptor, whereas D126A interaction activates the receptor. Strong interaction with F261/F284 lessens receptor activation, leading to antagonism (Figure 8B). Conversely, strong interaction with D126 enhances receptor activation, leading to agonism (Figure 8A). This model could be utilized to guide future development of agonists and antagonists. Agonism would be promoted by incorporating basic groups on the right-hand side of the compound to interact strongly with D126, while incorporating groups at the phenyl position that interact less strongly with the hydrophobic cage. Conversely, antagonist ligands could be developed by minimizing ligand interaction with D126 and by incorporating groups at the phenyl position that optimize interaction with the hydrophobic cage.

In conclusion, we have identified several determinants of nonpeptide ligand binding to the MC4 receptor and, for the first time, provide experimental evidence for interactions between amino acid side chains of the receptor and functional groups of nonpeptide ligand. These interactions are consistent with a molecular model of the MC4 receptor and provide experimental support for peptide mimicry by nonpeptide ligand. Differential effects of the mutations were observed between nonpeptide agonists and antagonists, suggesting that the differential strength of the interactions controls the signaling efficacy of the ligand. These findings will be useful for aiding the future design and differentiation of nonpeptide agonists and antagonists targeting the MC4 receptor.

ACKNOWLEDGMENT

The authors thank R. Scott Struthers for data interpretation and critical reading of the manuscript.

REFERENCES

1. Gantz, I., Konda, Y., Tashiro, T., Shimoto, Y., Miwa, H., Munzert, G., Watson, S. J., DelValle, J., and Yamada, T. (1993) Molecular cloning of a novel melanocortin receptor, *J. Biol. Chem. 268*, 8246−8250.
2. Gantz, I., Miwa, H., Konda, Y., Shimoto, Y., Tashiro, T., Watson, S. J., DelValle, J., and Yamada, T. (1993) Molecular cloning, expression, and gene localization of a fourth melanocortin receptor, *J. Biol. Chem. 268*, 15174−15179.
3. Mountjoy, K. G., Robbins, L. S., Mortrud, M. T., and Cone, R. D. (1992) The cloning of a family of genes that encode the melanocortin receptors, *Science 257*, 1248−1251.
4. Eipper, B. A., and Mains, R. E. (1980) Structure and biosynthesis of pro-adrenocorticotropin/endorphin and related peptides, *Endocr. Rev. 1*, 1−27.
5. Smith, A. I., and Funder, J. W. (1988) Proopiomelanocortin processing in the pituitary, central nervous system, and peripheral tissues, *Endocr. Rev. 9*, 159−179.
6. Irani, B. G., Holder, J. R., Todorovic, A., Wilczynski, A. M., Joseph, C. G., Wilson, K. R., and Haskell-Luevano, C. (2004) Progress in the development of melanocortin receptor selective ligands, *Curr. Pharm. Des. 10*, 3443−3479.
7. Lu, D., Willard, D., Patel, I. R., Kadwell, S., Overton, L., Kost, T., Luther, M., Chen, W., Woychik, R. P., Wilkison, W. O., et al. (1994) Agouti protein is an antagonist of the melanocyte-stimulating-hormone receptor, *Nature 371*, 799−802.
8. Yang, Y. K., Thompson, D. A., Dickinson, C. J., Wilken, J., Barsh, G. S., Kent, S. B., and Gantz, I. (1999) Characterization of Agouti-related protein binding to melanocortin receptors, *Mol. Endocrinol. 13*, 148−155.
9. Fong, T. M., Mao, C., MacNeil, T., Kalyani, R., Smith, T., Weinberg, D., Tota, M. R., and Van der Ploeg, L. H. (1997) ART (protein product of agouti-related transcript) as an antagonist of MC-3 and MC-4 receptors, *Biochem. Biophys. Res. Commun. 237*, 629−631.
10. Foster, A. C., Joppa, M., Markison, S., Gogas, K. R., Fleck, B. A., Murphy, B. J., Wolff, M., Cismowski, M. J., Ling, N., Goodfellow, V. S., Chen, C., Saunders, J., and Conlon, P. J. (2003) Body weight regulation by selective MC4 receptor agonists and antagonists, *Ann. N. Y. Acad. Sci. 994*, 103−110.
11. Gantz, I., and Fong, T. M. (2003) The melanocortin system, *Am. J. Physiol. Endocrinol. Metab. 284*, E468−474.
12. Fotsch, C., Han, N., Arasasingham, P., Bo, Y., Carmouche, M., Chen, N., Davis, J., Goldberg, M. H., Hale, C., Hsieh, F. Y., Kelly, M. G., Liu, Q., Norman, M. H., Smith, D. M., Stec, M., Tamayo, N., Xi, N., Xu, S., Bannon, A. W., and Baumgartner, J. W. (2005) Melanocortin subtype-4 receptor agonists containing a piperazine core with substituted aryl sulfonamides, *Bioorg. Med. Chem. Lett. 15*, 1623−1627.
13. Cepoi, D., Phillips, T., Cismowski, M., Goodfellow, V. S., Ling, N., Cone, R. D., and Fan, W. (2004) Assessment of a small molecule melanocortin-4 receptor-specific agonist on energy homeostasis, *Brain Res. 1000*, 64−71.
14. Benoit, S. C., Schwartz, M. W., Lachey, J. L., Hagan, M. M., Rushing, P. A., Blake, K. A., Yagaloff, K. A., Kurylko, G., Franco, L., Danhoo, W., and Seeley, R. J. (2000) A novel selective melanocortin-4 receptor agonist reduces food intake in rats and mice without producing aversive consequences, *J. Neurosci. 20*, 3442−3448.
15. Pan, K., Scott, M. K., Lee, D. H., Fitzpatrick, L. J., Crooke, J. J., Rivero, R. A., Rosenthal, D. I., Vaidya, A. H., Zhao, B., and Reitz, A. B. (2003) 2,3-Diaryl-5-anilino[1,2,4]thiadiazoles as melanocortin MC4 receptor agonists and their effects on feeding behavior in rats, *Bioorg. Med. Chem. 11*, 185−192.
16. Sebhat, I. K., Martin, W. J., Ye, Z., Barakat, K., Mosley, R. T., Johnston, D. B., Bakshi, R., Palucki, B., Weinberg, D. H., MacNeil, T., Kalyani, R. N., Tang, R., Stearns, R. A., Miller, R.

R., Tamvakopoulos, C., Strack, A. M., McGowan, E., Cashen, D. E., Drisko, J. E., Hom, G. J., Howard, A. D., MacIntyre, D. E., van der Ploeg, L. H., Patchett, A. A., and Nargund, R. P. (2002) Design and pharmacology of *N*-[(3*R*)-1,2,3,4-tetrahydroisoquinolinium- 3-ylcarbonyl]-(1*R*)-1-(4-chlorobenzyl)- 2-[4-cyclohexyl-4-(1H-1,2,4-triazol- 1-ylmethyl)piperidin-1-yl]-2-oxoethylamine (1), a potent, selective, melanocortin subtype-4 receptor agonist, *J. Med. Chem. 45*, 4589−4593.

17. Martin, W. J., and MacIntyre, D. E. (2004) Melanocortin receptors and erectile function, *Eur. Urol. 45*, 706−713.
18. Wessells, H., Fuciarelli, K., Hansen, J., Hadley, M. E., Hruby, V. J., Dorr, R., and Levine, N. (1998) Synthetic melanotropic peptide initiates erections in men with psychogenic erectile dysfunction: double-blind, placebo controlled crossover study, *J. Urol. 160*, 389−393.
19. Pfaus, J. G., Shadiack, A., Van Soest, T., Tse, M., and Molinoff, P. (2004) Selective facilitation of sexual solicitation in the female rat by a melanocortin receptor agonist, *Proc. Natl. Acad. Sci. U.S.A. 101*, 10201−10204.
20. Vos, T. J., Caracoti, A., Che, J. L., Dai, M., Farrer, C. A., Forsyth, N. E., Drabic, S. V., Horlick, R. A., Lamppu, D., Yowe, D. L., Balani, S., Li, P., Zeng, H., Joseph, I. B., Rodriguez, L. E., Maguire, M. P., Patane, M. A., and Claiborne, C. F. (2004) Identification of 2-[2-[2-(5-bromo-2- methoxyphenyl)-ethyl]-3-fluorophenyl]-4,5-dihydro-1H-imidazole (ML00253764), a small molecule melanocortin 4 receptor antagonist that effectively reduces tumor-induced weight loss in a mouse model, *J. Med. Chem. 47*, 1602−1604.
21. Joppa, M. A., Ling, N., Chen, C., Gogas, K. R., Foster A. C., and Markison, S. (2005) Central administration of peptide and small molecule MC4 receptor antagonists induce hyperphagia in mice and attenuate cytokine-induced anorexia, *Peptides*, in press.
22. Markison, S., Foster, A. C., Chen, C., Brookhart, G. B., Hesse, A., Hoare, S. R., Fleck, B. A., Brown, B. T., and Marks, D. L. (2005) The regulation of feeding and metabolic rate and the prevention of murine cancer cachexia with a small-molecule melanocortin-4 receptor antagonist, *Endocrinology 146*, 2766−2773.
23. Farooqi, I. S., Keogh, J. M., Yeo, G. S., Lank, E. J., Cheetham, T., and O'Rahilly, S. (2003) Clinical spectrum of obesity and mutations in the melanocortin 4 receptor gene, *N. Engl. J. Med. 348*, 1085−1095.
24. Coll, A. P., Farooqi, I. S., Challis, B. G., Yeo, G. S., and O'Rahilly, S. (2004) Proopiomelanocortin and energy balance: insights from human and murine genetics, *J. Clin. Endocrinol. Metab. 89*, 2557−2562.
25. Foster, A. C., Chen, C., Markison, S., and Marks, D. L. (2005) MC4 receptor antagonists: a potential treatment for cachexia, *IDrugs 8*, 314−319.
26. Marks, D. L., Ling, N., and Cone, R. D. (2001) Role of the central melanocortin system in cachexia, *Cancer Res. 61*, 1432−1438.
27. Holder, J. R., and Haskell-Luevano, C. (2004) Melanocortin ligands: 30 years of structure−activity relationship (SAR) studies, *Med. Res. Rev. 24*, 325−356.
28. Haskell-Luevano, C., Cone, R. D., Monck, E. K., and Wan, Y. P. (2001) Structure activity studies of the melanocortin-4 receptor by in vitro mutagenesis: identification of agouti-related protein (AGRP), melanocortin agonist and synthetic peptide antagonist interaction determinants, *Biochemistry 40*, 6164−6179.
29. Yang, Y. K., Fong, T. M., Dickinson, C. J., Mao, C., Li, J. Y., Tota, M. R., Mosley, R., Van Der Ploeg, L. H., and Gantz, I. (2000) Molecular determinants of ligand binding to the human melanocortin-4 receptor, *Biochemistry 39*, 14900−14911.
30. Nickolls, S. A., Cismowski, M. I., Wang, X., Wolff, M., Conlon, P. J., and Maki, R. A. (2003) Molecular determinants of melanocortin 4 receptor ligand binding and MC4/MC3 receptor selectivity, *J. Pharmacol. Exp. Ther. 304*, 1217−1227.
31. Wilczynski, A., Wang, X. S., Joseph, C. G., Xiang, Z., Bauzo, R. M., Scott, J. W., Sorensen, N. B., Shaw, A. M., Millard, W. J., Richards, N. G., and Haskell-Luevano, C. (2004) Identification of putative agouti-related protein(87−132)-melanocortin-4 receptor interactions by homology molecular modeling and validation using chimeric peptide ligands, *J. Med. Chem. 47*, 2194−2207.
32. Chai, B. X., Pogozheva, I. D., Lai, Y. M., Li, J. Y., Neubig, R. R., Mosberg, H. I., and Gantz, I. (2005) Receptor-antagonist interactions in the complexes of agouti and agouti-related protein with human melanocortin 1 and 4 receptors, *Biochemistry 44*, 3418−3431.
33. Haskell-Luevano, C., Holder, J. R., Monck, E. K., and Bauzo, R. M. (2001) Characterization of melanocortin NDP-MSH agonist peptide fragments at the mouse central and peripheral melanocortin receptors, *J. Med. Chem. 44*, 2247−2252.
34. Sawyer, T. K., Sanfilippo, P. J., Hruby, V. J., Engel, M. H., Heward, C. B., Burnett, J. B., and Hadley, M. E. (1980) 4-Norleucine, 7-D-phenylalanine-alpha-melanocyte-stimulating hormone: a highly potent alpha-melanotropin with ultralong biological activity, *Proc. Natl. Acad. Sci. U.S.A. 77*, 5754−5758.
35. Al-Obeidi, F., Castrucci, A. M., Hadley, M. E., and Hruby, V. J. (1989) Potent and prolonged acting cyclic lactam analogues of alpha-melanotropin: design based on molecular dynamics, *J. Med. Chem 32*, 2555−2561.
36. Bednarek, M. A., Macneil, T., Kalyani, R. N., Tang, R., Van der Ploeg, L. H., and Weinberg, D. H. (1999) Analogs of MTII, lactam derivatives of alpha-melanotropin, modified at the N-terminus, and their selectivity at human melanocortin receptors 3, 4, and 5, *Biochem. Biophys. Res. Commun. 261*, 209−213.
37. Hruby, V. J., Lu, D., Sharma, S. D., Castrucci, A. L., Kesterson, R. A., al-Obeidi, F. A., Hadley, M. E., and Cone, R. D. (1995) Cyclic lactam alpha-melanotropin analogues of Ac-Nle4-cyclo-[Asp5, D-Phe7, Lys10] alpha-melanocyte-stimulating hormone-(4−10)-NH_2 with bulky aromatic amino acids at position 7 show high antagonist potency and selectivity at specific melanocortin receptors, *J. Med. Chem. 38*, 3454−3461.
38. Bednarek, M. A., MacNeil, T., Kalyani, R. N., Tang, R., Van der Ploeg, L. H., and Weinberg, D. H. (2001) Selective, high affinity peptide antagonists of alpha-melanotropin action at human melanocortin receptor 4: their synthesis and biological evaluation in vitro, *J. Med. Chem. 44*, 3665−3672.
39. Chen, C., Pontillo, J., Fleck, B. A., Gao, Y., Wen, J., Tran, J. A., Tucci, F. C., Marinkovic, D., Foster, A. C., and Saunders, J. (2004) 4-{(2*R*)-[3-Aminopropionylamido]-3-(2,4-dichlorophenyl)propionyl}-1-{2-[(2-thienyl)ethylaminomethyl]phenyl}piperazine as a potent and selective melanocortin-4 receptor antagonist− design, synthesis, and characterization, *J. Med. Chem. 47*, 6821−6830.
40. Sun, H., Greeley, D. N., Chu, X. J., Cheung, A., Danho, W., Swistok, J., Wang, Y., Zhao, C., Chen, L., and Fry, D. C. (2004) A predictive pharmacophore model of human melanocortin-4 receptor as derived from the solution structures of cyclic peptides, *Bioorg. Med. Chem. 12*, 2671−2677.
41. Mutulis, F., Yahorava, S., Mutule, I., Yahorau, A., Liepinsh, E., Kopantshuk, S., Veiksina, S., Tars, K., Belyakov, S., Mishnev, A., Rinken, A., and Wikberg, J. E. (2004) New substituted piperazines as ligands for melanocortin receptors. Correlation to the X-ray structure of "THIQ", *J. Med. Chem. 47*, 4613−4626.
42. Pontillo, J., Tran, J. A., Fleck, B. A., Marinkovic, D., Arellano, M., Tucci, F. C., Lanier, M., Nelson, J., Parker, J., Saunders, J., Murphy, B., Foster, A. C., and Chen, C. (2004) Piperazinebenzylamines as potent and selective antagonists of the human melanocortin-4 receptor, *Bioorg. Med. Chem. Lett. 14*, 5605−5609.
43. Pontillo, J., Tran, J. A., Arellano, M., Fleck, B. A., Huntley, R., Marinkovic, D., Lanier, M., Nelson, J., Parker, J., Saunders, J., Tucci, F. C., Jiang, W., Chen, C. W., White, N. S., Foster, A. C., and Chen, C. (2004) Structure−activity relationships of piperazinebenzylamines as potent and selective agonists of the human melanocortin-4 receptor, *Bioorg. Med. Chem. Lett. 14*, 4417−4423.
44. Richardson, T. I., Ornstein, P. L., Briner, K., Fisher, M. J., Backer, R. T., Biggers, C. K., Clay, M. P., Emmerson, P. J., Hertel, L. W., Hsiung, H. M., Husain, S., Kahl, S. D., Lee, J. A., Lindstrom, T. D., Martinelli, M. J., Mayer, J. P., Mullaney, J. T., O'Brien, T. P., Pawlak, J. M., Revell, K. D., Shah, J., Zgombick, J. M., Herr, R. J., Melekhov, A., Sampson, P. B., and King, C. H. (2004) Synthesis and structure−activity relationships of novel arylpiperazines as potent and selective agonists of the melanocortin subtype-4 receptor, *J. Med. Chem. 47*, 744−755.
45. Arasasingham, P. N., Fotsch, C., Ouyang, X., Norman, M. H., Kelly, M. G., Stark, K. L., Karbon, B., Hale, C., Baumgartner, J. W., Zambrano, M., Cheetham, J., and Tamayo, N. A. (2003) Structure−activity relationship of (1-aryl-2-piperazinylethyl)-piperazines: antagonists for the AGRP/melanocortin receptor binding, *J. Med. Chem. 46*, 9−11.
46. Herpin, T. F., Yu, G., Carlson, K. E., Morton, G. C., Wu, X., Kang, L., Tuerdi, H., Khanna, A., Tokarski, J. S., Lawrence, R. M., and Macor, J. E. (2003) Discovery of tyrosine-based potent and selective melanocortin-1 receptor small-molecule agonists with anti-inflammatory properties, *J. Med. Chem. 46*, 1123−1126.

47. Marsilje, T. H., Roses, J. B., Calderwood, E. F., Stroud, S. G., Forsyth, N. E., Blackburn, C., Yowe, D. L., Miao, W., Drabic, S. V., Bohane, M. D., Scott Daniels, J., Li, P., Wu, L., Patane, M. A., and Claiborne, C. F. (2004) Synthesis and biological evaluation of imidazole-based small molecule antagonists of the melanocortin 4 receptor (MC4−R), *Bioorg. Med. Chem. Lett. 14*, 3721−3725.
48. Lapinsh, M., Veiksina, S., Uhlen, S., Petrovska, R., Mutule, I., Mutulis, F., Yahorava, S., Prusis, P., and Wikberg, J. E. (2005) Proteochemometric mapping of the interaction of organic compounds with melanocortin receptor subtypes, *Mol. Pharmacol. 67*, 50−59.
49. Lapinsh, M., Prusis, P., Mutule, I., Mutulis, F., and Wikberg, J. E. (2003) QSAR and proteo-chemometric analysis of the interaction of a series of organic compounds with melanocortin receptor subtypes, *J. Med. Chem. 46*, 2572−2579.
50. Yang, X., Wang, Z., Dong, W., Ling, L., Yang, H., and Chen, R. (2003) Modeling and docking of the three-dimensional structure of the human melanocortin 4 receptor, *J. Protein Chem. 22*, 335−344.
51. Bondensgaard, K., Ankersen, M., Thogersen, H., Hansen, B. S., Wulff, B. S., and Bywater, R. P. (2004) Recognition of privileged structures by G-protein coupled receptors, *J. Med. Chem. 47*, 888−899.
52. Tucci, F. C., White, N. S., Markison, S., Joppa, M., Tran, J. A., Fleck, B. A., Madan, A., Dyck, B. P., Parker, J., Pontillo, J., Arellano, L. M., Marinkovic, D., Jiang, W., Chen, C. W., Gogas, K. R., Goodfellow, V. S., Saunders, J., Foster, A. C., Chen, C. (2005) Potent and orally active non-peptide antagonists of the human melanocortin-4 receptor based on a series of trans-2-disubstituted cyclohexylpiperazines, *Bioorg. Med. Chem. Lett. 15*, 4389−4395.
53. Hoare, S. R., Sullivan, S. K., Ling, N., Crowe, P. D., and Grigoriadis, D. E. (2003) Mechanism of corticotropin-releasing factor type I receptor regulation by nonpeptide antagonists, *Mol. Pharmacol. 63*, 751−765.
54. Cheng, Y., and Prusoff, W. H. (1973) Relationship between the inhibition constant (K1) and the concentration of inhibitor which causes 50% inhibition (I50) of an enzymatic reaction, *Biochem. Pharmacol. 22*, 3099−3108.
55. Arunlakshana, O., and Schild, H. O. (1959) Some quantitative uses of drug antagonists, *Br. J. Pharmacol. 14*, 48−58.
56. Strange, P. G. (1996) The energetics of ligand binding at catecholamine receptors, *Trends Pharmacol. Sci. 17*, 238−244.
57. Palczewski, K., Kumasaka, T., Hori, T., Behnke, C. A., Motoshima, H., Fox, B. A., Le Trong, I., Teller, D. C., Okada, T., Stenkamp, R. E., Yamamoto, M., and Miyano, M. (2000) Crystal structure of rhodopsin: A G protein-coupled receptor, *Science 289*, 739−745.
58. Gether, U., and Kobilka, B. K. (1998) G protein-coupled receptors. II. Mechanism of agonist activation, *J. Biol. Chem. 273*, 17979−17982.
59. Ballesteros, J. A., Shi, L., and Javitch, J. A. (2001) Structural mimicry in G protein-coupled receptors: implications of the high-resolution structure of rhodopsin for structure−function analysis of rhodopsin-like receptors, *Mol. Pharmacol. 60*, 1−19.
60. Holder, J. R., Xiang, Z., Bauzo, R. M., and Haskell-Luevano, C. (2002) Structure−activity relationships of the melanocortin tetrapeptide Ac-His-D-Phe-Arg-Trp-NH_2 at the mouse melanocortin receptors. 4. Modifications at the Trp position, *J. Med. Chem. 45*, 5736−5744.
61. Ballesteros, J. A., and Weinstein, H. (1995) Integrated methods for the construction of three-dimensional models of structure−function relations in G protein-coupled receptors, *Methods Neurosci. 25*, 366−428.

BI051316S